Available online at www.sciencedirect.com
ScienceDirect
ELSEVIER
Palaeogeography, Palaeoclimatology, Palaeoecology 240 (2006) 275–304
PALAEO
www.elsevier.com/locate/palaeo

Characterisation of non-extractable macromolecular organic matter in Palaeozoic coals

Jens Wollenweber [a], Jan Schwarzbauer [a,*], Ralf Littke [a], Heinz Wilkes [b], Antje Armstroff [c], Brian Horsfield [b]

[a] *Lehrstuhl für Geologie, Geochemie und Lagerstätten des Erdöls und der Kohle, RWTH Aachen, Lochnerstrasse 4-20, 52056 Aachen, Germany*
[b] *Organische Geochemie, GeoForschungsZentrum Potsdam, 14473 Potsdam, Germany*
[c] *Institut für Sedimentäre Systeme, Forschungszentrum Jülich GmbH, 52425 Jülich, Germany*

Received 15 March 2005; accepted 24 March 2006

Abstract

Comprehensive organic–geochemical investigations were applied to Permian, Carboniferous and Devonian coals. The major goal of the investigation was to quantify differences in organic matter composition of the coals on a molecular level and to associate these differences with either i) primary composition of the precursor plant material, or ii) diagenetic processes related to burial and temperature increase or iii) evolutionary time trends.

The pre-extracted samples were analysed by means of pyrolytic and chemical degradation techniques as well as FTIR spectroscopy. Additionally, Rock-Eval pyrolysis and organic petrography were used to obtain information on the bulk of the coal samples.

The degradation analysis revealed a wide variety of individual compounds including *n*-alkanes, isoprenoids, polycylic aromatic compounds, fatty acids, alkylbenzenes, aromatic carboxylic acids and phenols. Relative concentrations of substances or compound groups were correlated with bulk parameters and age of the samples.

Significant correlations of the chemical data were found out mainly for maturity parameters and maceral composition. Time depending changes in chemical composition were observed only to a minor extent. Thus, the rapid morphologic evolution of higher land plants in the Late Palaeozoic is not reflected in a significant way by the chemical composition of the non-extractable matter in the coal samples investigated.
© 2006 Elsevier B.V. All rights reserved.

Keywords: Macromolecular organic matter; Infrared spectra; Palaeozoic; Plant evolution; Thermal maturity; Pyrolysis; Chemical degradation

1. Introduction

The origin and early diversification of land plants in the Palaeozoic marks an interval of unparalleled innovation in the history of plant life. From a simple plant body consisting only of a few cells, land plants evolved and elaborated two-phase life cycle and an extraordinary array of complex organs and tissue systems. Specialized sexual organs, stems with an intricate fluid transport mechanism, structural tissues, epidermal structures for respiratory gas exchange, leaves and roots of various kinds, diverse spore-bearing organs and seeds had all evolved during the Devonian period (Meyer-Berthaud et al., 1999). These and other innovations led to the initial assembly of plant-dominated terrestrial ecosystems, and had a great effect on the global environment.

* Corresponding author. Tel.: +49 241 8095750; fax: +49 241 80695750.
E-mail address: schwarzbauer@lek.rwth-aachen.de
(J. Schwarzbauer).

0031-0182/$ - see front matter © 2006 Elsevier B.V. All rights reserved.
doi:10.1016/j.palaeo.2006.03.053

The phytoterrestrialization by plants is closely linked with morphological modifications and the development of specific biochemical accoutrements. The adaptation of land plants based mainly on the physico-chemical properties of the macromolecular components in the specialized tissues and organs. For example the cuticular matrix was build up as desiccation inhibitors dominantly consisting of the polyester cutin partially accompanied by the polymer cutan. For the protection of seeds in soils a structurally related biopolymer, suberin, is used by land plants, that is also occurring in further tissues like cork and root periderm layer. A similar function is fulfilled by the biopolymer sporopollenin, which is an important chemical constituent of spores and pollen. Furthermore, the development of stems and associated water conductive tracheids and supporting systems in arborescent plants is closely linked with lignin, a polymerisation product of *p*-coumaryl alcohol, coniferyl alcohol and sinapyl alcohol in variable proportions.

Organic matter derived from Palaeozoic land plants is chemically best preserved in coals and related material. However, the major part of plant components in coals is degraded during coalification as the result of thermal stress and only the more resistant fraction survives (Tegelaar et al., 1989). From a geochemical point of view the more resistant part consists of numerous low molecular weight compounds as well as of macromolecular organic matter. A sub-fraction of these substances conserves its major structural properties of biogenic origin and, therefore, can act as chemical fossils or biomarkers in geochemical studies. This approach is widely used for the low molecular weight substances especially in Palaeozoic coals (e.g. Schulze and Michaelis, 1989; Moldowan et al., 1994; Fabianska and Kruszewska, 2003), but it is applied to the geopolymers only to a minor extend (e.g. Nip et al., 1986).

Principally, detailed chemical information on coaly organic matter of high molecular weight can be obtained either by non-destructive methods, in particular analyses by NMR or IR spectroscopy (e.g. Nip et al., 1986; Béhar and Hatcher, 1995; Mastalerz et al., 1998; Garcette-Lepecq et al., 2000; Riboulleau et al., 2000; Zodrow et al., 2000; Simpson and Hatcher, 2004), or after considerable modification of the macromolecular organic matter by chemical or pyrolytic degradation methods (e.g. ten Haven et al., 1992; Han and Kruge, 1999; Disnar and Harouna, 1994) and subsequent analyses of the low molecular weight products. A review focusing on these analytical approaches has been recently published for soil organic matter (Kögel-Knabner, 2000).

Analytical pyrolysis is another way to analyse kerogen, coal, peat, humic substances, soil or wood. Different procedures are usually applied including on-line and off-line methods, with or without derivatisation of the products and subsequent gas chromatographic or gas chromatographic–mass spectrometric (GC–MS) analysis (e.g. Bracewell and Robertson, 1980; Horsfield, 1989; Schenk et al., 1990; Béhar and Hatcher, 1995; Galletti and Bocchini, 1995; Schulten and Leinweber, 1995; Stankiewicz et al., 1996; Mösle et al., 1997; Mongenot et al., 1999). In contrast, appropriate chemical degradation procedures allow the selective release of components depending on the mode of binding. Common degradation reactions include acidic hydrolysis (e.g. Cranwell, 1981; Grasset and Amblès, 1998), alkaline hydrolysis (Naafs and van Bergen, 2002), ether and ester cleavages using strong acids like boron trihalides or hydroiodic acid (e.g. Jenisch et al., 1990; Vella and Holzer, 1990; Richnow et al., 1994; Gelin et al., 1997; Ping'an Peng et al., 1997) or oxidation e.g. with CuO or RuO_4 (e.g. Hedges and Mann, 1979; Myke and Michaelis, 1986; Choi et al., 1988; Blanc and Albrecht, 1990; Goni et al., 1993; Camarero et al., 1994; Orem et al., 1997). The degradation products were usually extracted, fractionated and analysed by LC, GC or GC–MS. Using a sequential degradation approach with an increasing order of reactivity, a differentiation of individual modes of binding can be achieved (Schwarzbauer et al., 2005).

Although investigations on the non-extractable organic fraction of Palaeozoic coals are limited, some of these analytical approaches were used to characterize macromolecular organic matter of Palaeozoic age. However, these studies focussed mainly on macrofossils. Ewbank et al. (1996) examined coalified residues of three vascular plants of the Devonian by pyrolysis coupled to GC–MS. By comparison of fossil samples with recent material they were able to demonstrate that selected biogenic macromolecules associated with higher land plants were partially preserved especially in samples of low maturity. In detail lignin and cutan related residues were revealed to be the major source of vascular plant derived organic material in these fossil samples. These macromolecules were mainly characterized by alkylated phenols and aromatic hydrocarbons or highly aliphatic pyrolysates, respectively. In particular the chemical evidence of cutan is the earliest one so far.

Furthermore, Mösle et al. (2002) performed chemosystematic investigations of different Late Carboniferous plants based on pyrolytic analysis of preserved cuticle material. Comparing the cuticle pyrolysates it was stated, that this fossil material retained some chemosytematic signatures. Also van Bergen et al. (1994) performed Curie-Point-pyrolsis and ^{13}C-NMR analyses on cuticles of pteridosperm genera derived from the Upper Carboniferous and characterized especially the aliphatic moieties of the most resistant constituents.

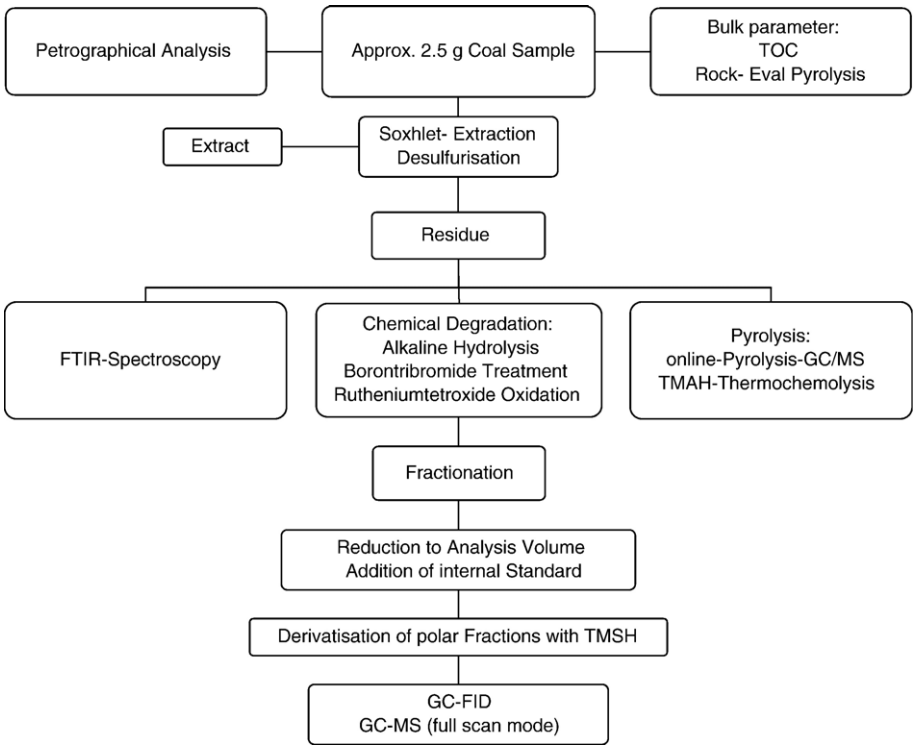

Fig. 1. Flow scheme of analytical procedures and microscopical methods applied in this work.

A combination of FTIR spectroscopy, pyrolysis and petrographic techniques was used by Mastalerz et al. (1998) to characterize a specific Devonian fossil, Protosalvinia, which obviously combined properties of aquatic and terrestrial plants. This was also found out by the chemical analyses representing on the one hand macromolecular structures similar to lignin, on the other hand aliphatic components related to marine organic matter. These observations were supported by maceral analysis revealing cutinite and alginite related contributions.

In addition to organic geochemical investigations on a molecular level, Palaeozoic coals were also characterized by bulk parameters and petrographical analyses. For example Littke and ten Haven (1989) and Veld et al. (1993) identified substantial differences between Westphalian coals in the vicinity of the Variscan deformation front and Littke et al. (1989) and Scheidt and Littke (1989) showed that the chemical preservation of terrestrial organic matter in coal seams is much better than in adjacent siltstones and sandstones, although the morphological preservation may be superior in the latter.

Nevertheless, the knowledge on plant derived macromolecular organic matter from the Palaeozoic is still very limited (e.g. van Bergen et al., 1994; Ewbank et al., 1996; Stankiewicz et al., 1998; Mösle et al., 2002), although land plant evolution was an important process during this time period. Consequently, the aim of this study was to examine the characteristics and the development of fossil macromolecular organic matter in coals from the Devonian to the Permian. In order to get a comprehensive view on the organic–chemical properties various complementary analytical methods were applied including pyrolysis, IR spectroscopy and chemical degradation techniques.

The major goal of the investigation was to quantify differences in organic matter composition of the coals on a molecular level and to associate these differences with either i) primary composition of the precursor plant material, or ii) diagenetic processes related to burial and temperature increase or iii) evolutionary time trends.

2. Material and methods

An overview on the analytical procedures and microscopical methods applied to the coal samples is given in Fig. 1.

2.1. Sample material

In summary 34 coal samples and 7 fossils were investigated. The age of the samples covers the time period between the Devonian (2 samples) and the Permian (9 samples), with a maximum sample number in the

Table 1

a. Summary of coal samples investigated and applied analytical techniques

Period	Series	Stage/formation	Sample no.	Country	Location	Depth [m]	Petrography	TOC	Rock-Eval pyrolysis	FTIR-spectroscopy	Pyrolysis	TMAH thermochemolysis	Chemical degradation
Permian													
	Upper Permian		CP1	Australia	Nipan o Seam, Bowen Basin		+	+	+	+	+	+	+
	Upper Permian		CP2	Australia	Upper Wynn, Sydney Basin		+	+	+	+	+	+	+
	Upper Permian		CP3	Australia	Bulli Seam, Sydney Basin		+	+	+	+	+	+	+
		Lower Zechstein	CP4	China	Dahe Mine		+	+	+		+	+	+
	Rotliegend		CP5	Russia	Petchora Basin		+	+	+	+	+	+	+
		Artinskian/ Kungarian	CP6	Brasilia	Rio Benito Formation		+	+	+	+	+	+	+
		Artinskian/ Kungarian	CP7	Brasilia	Rio Benito Formation		+	+	+	+	+	+	+
	Lower Permian		CP8	Antarctica	Heimefrontfjella		+	+	+		+	+	+
Carboniferous													
	Westphalian	Westphalian D	CC1	Germany	Vertrauensflöz			+			+	+	
		Westphalian C	CC2	England	Keekle 2194			+			+		+
		Westphalian B	CC3	England	Potato Pot	24.7	+	+	+	+	+	+	+
		Westphalian B	CC4	England	Potato Pot	25.5	+	+	+	+		+	+
		Westphalian B	CC5	England	Potato Pot	29.5	+	+	+	+	+		+
		Westphalian B	CC6	England	Potato Pot	29.9	+	+	+	+	+		+
		Westphalian A	CC7	England	Rowland Gill	51.6	+	+	+		+		
		Westphalian A	CC8	England	Potato Pot	59.6	+	+	+	+	+	+	+
		Westphalian A	CC9	England	Potato Pot	59.8	+	+	+			+	+
		Westphalian A	CC10	England	Potato Pot	63.9	+	+	+	+		+	+
		Westphalian A	CC11	England	Potato Pot	77.9	+	+	+	+	+	+	+
		Westphalian A	CC12	England	Potato Pot	78.3	+	+	+	+			+
		Westphalian A	CC13	England	Distington I	12.9	+	+			+	+	+
	Namurian		CC14	England	Dearham	45.1		+	+				+
	Namurian		CC15	England	Dearham	44.8	+	+	+	+	+		+
	Namurian		CC16	England	Dearham	55.3	+	+	+	+	+	+	+
	Namurian		CC17	England	Dearham	56.3		+	+			+	
	Namurian		CC18	England	Rowland Gill	93.8	+	+	+	+			
	Viséan		CC19	Russia	Moscow Basin		+	+	+	+	+		
	Viséan		CC20	Russia	Moscow Basin		+	+	+	+			

	Viséan		CC21	Russia	Moscow Basin	+		+	+	+	+	+	+
	Viséan		CC22	Germany	Borna Hainichen	+		+	+	+	+		
	Viséan		CC23	Russia	Moscow Basin	+		+	+	+	+	+	+
	Viséan		CC24	Russia	Moscow Basin	+		+	+	+	+	+	+
	Lower Viséan		CC25	Spitsbergen	Mumien	+		+	+	+	+		
Devonian													
	Upper Devonian	Givetium–Frasnium	CD1	Spitsbergen	Mimerdalen	+		+		+	+	+	+

b. Summary of fossils investigated and applied analytical techniques

Period	Series	Samplev no.	Location	Origin	Flora realm	Petrography	TOC	Rock-Eval pyrolysis	FTIR-spectroscopy	Pyrolysis	TMAH-thermochemolysis	Chemical degradation
Permian												
	Lower Permian	FP1	Tansania	Glossopteris	Gondwana	+	+	+		+	+	+
Carboniferous												
	Upper Carboniferous	FC1	England	Coal Ball	Euramerian–cataysian	+	+	+		+		+
	Upper Carboniferous	FC2	England	Lepidodendron	Euramerian–cataysian	+	+	+		+	+	+
	Lower Carboniferous	FC3	Russia	Paper Coal	Euramerian–cataysian	+		+		+	+	+
	Lower Carboniferous	FC4	Russia	Lepidodendron	Euramerian–cataysian	+				+	+	+
	Lower Carboniferous	FC5	Russia	Lycopod-spores	Euramerian–cataysian	+	+			+	+	+
Devonian												
	Lower Devonian	FD1	Germany	Bad Münstereifel/ Brandschiefer	Euramerian (Psilophyta-province)	+	+	+		+	+	+

Carboniferous (30 samples). In Table 1a+b all samples and the analytical methods applied to the individual specimen are summarized. Information on the extractable organic matter as well as additional palaeogeographic information is presented in Armstroff et al., 2006-this volume.

Due to the aim of this work it was necessary to investigate samples of low maturity. Furthermore, the organic matter should have been well preserved which is the case in swamps or bogs. It was impossible to receive a complete sample series of this quality from one locality which comprises the entire Late Palaeozoic. Hence the coal samples originate from different locations.

The majority (17) of the coal samples investigated originate from the Pennine Basin in North England, located north of the Variscan deformation front. Geographically, they are from Cumberland, Durham and Northumberland. Stratigraphically, they represent different intervals of the Namurian and Westphalian when tropical forests persisted in the area.

One of the sample sets originates from the Moscow Basin. All five samples are of Viséan age, when much organic material was deposited in the southern part of the Moscow Basin (Alekseev et al., 1996).

Another two coal samples originate from Spitzbergen and were deposited in tropical environments. They represent the oldest samples investigated. One is ascribed to the Mimerdalen formation/Dickson Land, deposited at the Givetium–Frasnium boundary. The second coal originates from the Mumien Formation and is ascribed to the Lower Viséan.

The two coals from Germany originate from Erzgebirge, Saxony, and were deposited in the Subvariscian fore deep. The first sample is ascribed to the Hainchen Formation and is of Viséan age. The second coal originates from the Westphalian D and is taken from the Zwickau Formation located in Zwickau–Oelnitz (Armstroff et al., 2006-this volume).

The three coals not belonging to the Euramerican flora realm is a sample from the Petchora Basin in Russia, a coal from Dahe Mine, Shuicheng Basin in Southwest China and one from Heimefrontfjella, Antarctica. The first coal was deposited in Permian time. The Petchora Basin contains a Permian flora different from the Euramerian flora (Chaloner and Meyen, 1973). The second sample was deposited in a paralic depositional system with marine influence (Zhong and Smyth, 1997) during Late Permian whereas the coal from Antarctica originates from Lower Permian. Geographically it is from Amelang Plateau Formation, located in western Dronning Maud Land.

Two other Permian samples are derived from the Rio Benito Formation in Brasila, located in the Parana Basin in the east of the Southern American Platform. They were deposited during Artinskian/Kungarian and indicate an origin in limno-telmatic mires in which hypoautochthonic pteridophytic arborescent and herbaceous plant rests were deposited (Silva and Kalkreuth, 2005).

The Permian sample set is completed by three coals from Australia, ascribed to the Late Permian. One sample originates from the Nipan o Seam in Bowen Basin, the other two from Sydney Basin, one from the Bulli Seam, the other from Upper Wynn. These samples do not belong to the Euramerian flora realm as well.

Besides the thirty four coals, seven fossils have been investigated. All fossils, except the fossils from Tansania, arise from the Euramerian–Cataysian flora realm.

The fossil from Rhenish Massif is of Emsian age and can be described as a carbonaceous shale rich in well-preserved spores of low thermal maturity. One fossil from Tansania represents the Lower Permian Gondwana Glossopteris flora.

Two other fossils originate from the Upper Carboniferous in England. The first fossil is a coal ball, composed of peat and dolomite. The second fossil is a Lepidodendron stem.

Three fossil-bearing rocks originate from the Moscow Basin and are of Early Carboniferous age. One is a Dysodil-brown coal (paper-coal) derived from Lepidodendrales. It contains remains of Eskaia (Collinson et al., 1994). The second fossil is as well ascribed to Lepidodendrales. The third fossil-bearing rocks contains abundant macrospores of Lycopods.

2.2. Petrography

Microscopical investigations were performed on polished sections cut perpendicular to bedding using a Zeiss Universal microscope. The reflectance of the organic particles was measured with a 50× immersion objective in monochromatic light (546 nm) using the standard method described by Taylor et al. (1998).

2.3. Bulk parameters

After crushing of the samples Total Organic Carbon contents (TOC) were determined using a Leco Carbon-Analyser IR-112. Rock-Eval pyrolyses were performed on a Rock-Eval II instrument according to the method of Espitalié et al. (1977). All determinations were carried out in duplicate.

2.4. Extraction

Prior to the analysis of the non-extractable organic matter all samples were pre-extracted by means of

Table 2
Single absorption bands and their corresponding denotation

Wavelength (cm^{-1})	Type of vibration	Denotation
3400	OH stretching	OH
3100–3000	Aromatic CH stretching	CH_{arom}
3000–2700	Aliphatic CH stretching	CH_{aliph}
1750–1640	Carbonyl C═O stretching	CO
1600–1500	Aromatic C═C stretching	CC_{arom}
1500–700	Overlap of various vibrations	Fingerprint

dispersion extraction using an azeotrope mixture of acetone, chloroform and methanol (30:47:23; w:w:w) in two successive steps. After separation of the crude extracts the residues were dried and transferred to the spectroscopic, pyrolytic and chemical degradation analysis.

Details on the extraction procedure as well as on the analyses of the extractable compounds are reported elsewhere (Armstroff et al., 2006-this volume).

2.5. FTIR spectroscopy

FTIR analyses of pre-extracted coal samples were performed on a Nicolet FT-IR 505 spectrometer. Aliquots of approx. 1 mg were used for preparation of KBr pellets. For the measurements the optical resolution was set to 4 cm^{-1} and 1024 scans were performed for each analysis. The peak assignment was based on published data (King et al., 1963; Erdmann, 1965a,b; Espitalié et al., 1973; Robin and Rouxhet, 1976; Guo and Bustin, 1998) and the absorption bands discussed are listed in Table 2. For the quantitative examination the software PC/IR (version 3.20) from Nicolet was used. Quantitative data of individual bands obtained by integration were normalized on the total absorption of the IR spectra. Specific IR absorption ratios within one spectrum were obtained by division of the corresponding areas integrated. Additionally, Fig. 2 exemplifies the specific absorption areas investigated and the corresponding denotation.

2.6. Pyrolysis

Pyrolytic analysis was applied to aliquots of approx. 10 mg of pre-extracted material by online pyrolysis-gas chromatography (Py-GC) as well as by online pyrolysis-gas chromatography-mass spectrometry (Py-GC–MS). Pyrolysis-gas chromatography was performed using a Horizon Curie-Point Pyrolysator with a pyrolysis temperature of 710 °C held for 10 s. The interface was heated to 300 °C and the capillary column was directly inserted into the pyrolysis chamber. The gas chromatographic separation was carried out on a GC 4100 gas chromatograph (Carlo Erba, Milano, I) equipped with a 25 m × 0.25 mm i. d. × 0.25 μm film SE52 fused silica capillary column (CS Chromatographie Service, Langerwehe, FRG). For Py-GC–MS analyses the same Pyrolysator device was linked to a HP5890 gas chromatograph (Hewlett Packard, Palo Alto, USA) which was equipped with a 30 m × 0.22 mm i. d. × 0.25 μm film BPX5 fused silica capillary column (SGE, Weiterstadt, FRG). Chromatographic conditions were: 1 μl split/splitless injection at 60 °C, splitless time 60 s, 3 min hold, then programmed at 3 °C/min to 300 °C, helium carrier gas velocity was 40 cm/s. The mass

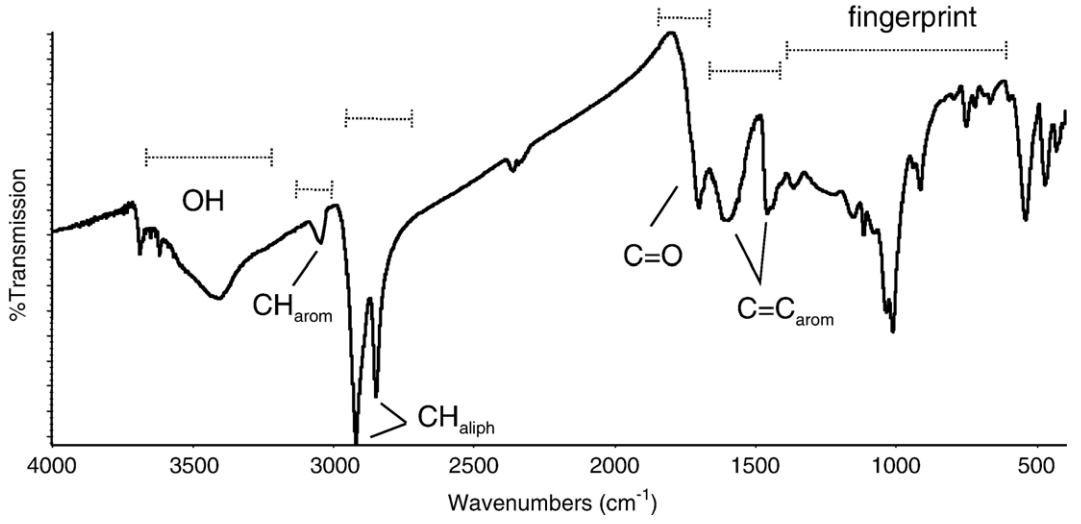

Fig. 2. Specific absorption areas and their corresponding denotation of a coal sample from Potato Pot, England (sample CC9).

Table 3
Identified compounds and their corresponding ion traces

Compound class	Group	Substances	Ions
Aliphatic hydrocarbons	Aliph	*n*-alkanes	85
		n-alkenes	83
		n-alkines	81
Polycyclic aromatic hydrocarbons	PAHs	Acenaphthylene	152
		Acenaphthene	154
		Fluorene	166
		Phenanthrene	178
		Anthracene	178
		Methylphenanthrenes	192
		Fluoranthene	202
		Pyrene	202
		Methylpyrenes/–fluoranthenes	216
Benzenes	Benz	Benzene	78
		Methylbenzenes	92
		C_2-benzenes	106
		C_3-benzenes	120
Oxygen containing compounds	Oxyg	Phenol	94
		Methylphenols	108
		C_2-phenols	122
		Dibenzofuran	168
		Long chain *n*-alkanoic acids (detected as methylesters)	74

spectrometric detection was carried out on a Finnigan MAT 8222 mass spectrometer (Finnigan, Bremen, FRG) which was operated at a resolution of 1000 in electron impact ionization mode (EI^+, 70 eV) with a source temperature of 200 °C scanning from 35 to 700 amu at a rate of 1 s/decade with an inter-scan time of 0.1 s.

The identified compounds were quantified by integration of specific ion chromatograms. All compounds determined and the corresponding ion chromatograms used are summarized in Table 3.

2.7. Tetramethylammonium hydroxide-thermochemolysis

Tetramethylammonium hydroxide (TMAH)-thermochemolysis was performed on approx. 20 mg pre-extracted samples placed in an ampoule with 500 µl of 25% methanolic TMAH solution. The suspension was reduced to a paste under a gentle stream of nitrogen. Thereafter the sample vials were sealed and placed in an oven programmed as follows: for 1 min held isothermally at 40 °C then heated up by a rate of 40 °C/min to 300 °C held isothermally for 10 min. After cooling down to room temperature the tube was cracked and the residue was extracted three times with 10 ml dichloromethane, respectively. The combined extracts were dried with anhydrous granulated sodium sulphate, taken up with *n*-pentane and separated into three fractions by column chromatography (Baker, 2 g silica gel 40 µm) using a mixture of dichloromethane and *n*-pentane (50:50 v:v; fraction 1), dichloromethane (fraction 2) and methanol (fraction 3) as the eluent, respectively. To each fraction 100 µl of an internal standard solution containing 42.3 ng/µL d_{10}-anthracene was added and the volume was reduced to 500 µl by rotary evaporation at room temperature.

2.8. Chemical degradation

Chemical degradation was applied to 26 coal samples and 7 fossils. Three degradation methods, alkaline hydrolysis, BBr_3-treatment and RuO_4-oxidation were applied to the samples in a sequential mode. In Fig. 3 the flow scheme of the analytical procedure is given.

2.8.1. Alkaline hydrolysis

Aliquots of 2.5 g of the pre-extracted samples were placed in 40 ml centrifuge-vials. 2.5 g of KOH dissolved in a mixture of 2 ml HPLC-grade water and 20 ml of

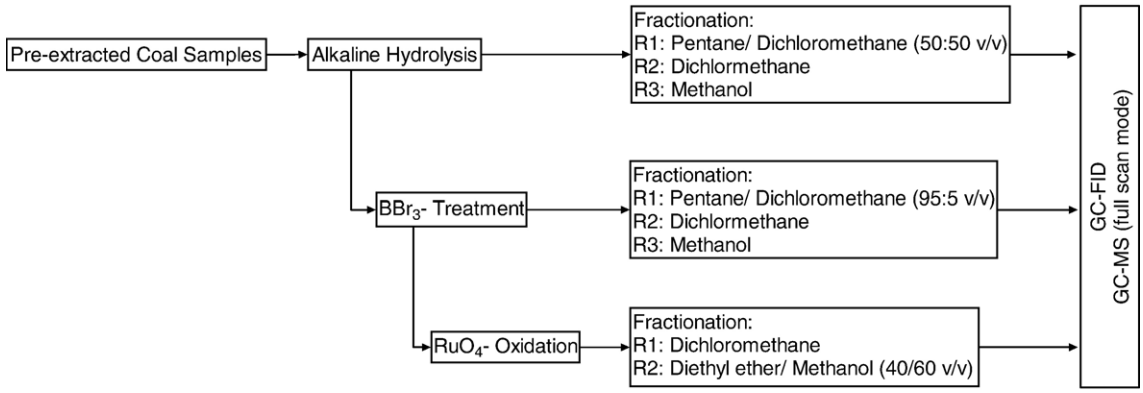

Fig. 3. Analytical flow scheme of the chemical degradation procedures.

methanol were added. Thereafter, the closed vials were treated by ultrasonication for 15 min and heated at 105 °C for 24 h. After cooling and centrifugation the liquid was decanted to a separatory funnel filled with 50 ml HPLC grade water. The residues were extracted in triplicate with 5 ml methanol, 5 ml acetone and 5 ml *n*-pentane, respectively. Each extraction step was followed by centrifugating and decanting or filtering using Whatman glass fiber filters (0.7 μm pore diameter). The combined extracts were added to the water phase in the separatory funnel and the mixture was acidified to pH 4–5 by addition of hydrochloric acid. Subsequently, the solution was extracted three times with 30 ml of dichloromethane. The combined organic layers were dried with anhydrous granulated sodium sulphate and concentrated to a volume of approx. 0.5 ml.

The crude extracts were separated into three fractions by column chromatography (Baker, 2 g silica gel 40 μm) using a mixture of dichloromethane and *n*-pentane (50:50; v:v; fraction 1), dichloromethane (fraction 2) and methanol (fraction 3) as the eluent, respectively. Prior to analysis, 50 μl of an internal standard containing 60 ng/μl d_{34}-hexadecane in *n*-hexane were added to each fraction, and the volume was reduced to 500 μl by rotary evaporation at room temperature.

2.8.2. BBr_3 treatment

To the residue of the hydrolysis samples 10 ml of a 1.0 M boron tribromide solution in dichloromethane was added. Following, ultrasonication in a water bath for 3 × 15 min was performed. After 24 h of stirring at room temperature a second ultrasonic treatment was applied, followed by another 24 h of stirring. Subsequently 10 ml of diethylether were added, the supernatant was decanted and filtered using a Whatman glass fiber filter (0.7 μm pore diameter). The solid residue was washed twice with diethylether and after filtration the combined organic solutions were added to the filtered reaction mixture. The combined organic layers were washed twice with 5 ml of pre-extracted water and dried with anhydrous granulated sodium sulphate. Prior to fractionation the solutions were concentrated to a volume of approx. 0.5 ml by rotary evaporation.

The crude extracts were separated into three fractions by column chromatography (Baker, 2 g silica gel 40 μm) using the following mixtures as the eluent: Fraction 1 — *n*-pentane/dichloromethane (95:5; v:v), fraction 2-dichloromethane, fraction 3 — methanol. Prior to analysis, 50 μl of an internal standard containing 60 ng/μl d_{34}-hexadecane in *n*-hexane were added to each fraction, and the volume was reduced to 500 μl by rotary evaporation at room temperature.

2.8.3. RuO_4-treatment

A mixture of 8 ml tetrachloromethane, 8 ml acetonitrile and 1 ml of pre-extracted water was added to the residues of the boron tribromide treatment. In addition, 500 mg sodium periodate and 10 mg of ruthenium tetroxide were added and the reaction mixture was stirred for 4 h in darkness. The reaction was stopped by addition of 50 μl of methane and 2 drops of concentrated sulphuric acid. The liquid phase was separated by decantation and the residue was extracted twice with 20 ml of tetrachloromethane. The combined organic layers were collected in a separatory funnel and washed with 5 ml of pre-extracted water as well as 1 ml of a sodium thiosulfate solution. All water layers were combined and re-extracted five times with 10 ml of diethylether. The diethylether solution was added to the organic solution, the extract was dried with anhydrous granulated sodium sulphate and concentrated to a volume of 0.5 ml prior to fractionation.

The crude extracts were separated into two fractions by column chromatography (Baker, 2 g silica gel 40 μm) using the following mixtures as the eluent: Fraction 1 — dichloromethane, fraction 2 — diethylether/methanol (40:60; v:v). Prior to analysis, 50 μl of an internal standard containing 60 ng/μl d_{34}-hexadecane in n-hexane was added to each fraction, and the volume was reduced to 500 μl by rotary evaporation at room temperature.

2.9. Derivatization of acidic compounds

Prior to GC and GC/MS analysis the acid compounds in the polar fractions (eluted with methanol) obtained from the chemical degradation procedures and the TMAH-thermochemolysis were methylated by addition of 5 μl of a TMSH solution to aliquots of 5 μl of the extracts. The mixture was ultrasonicated for 5 min and the volume was reduced to approx. 2 μl. The total solution was injected into the gas chromatograph.

It has to be noted, that during TMAH thermochemolysis the methylation of the products is not necessarily complete according to Quénéa et al. (2005). Hence a second methylation of acidic compounds based on TMSH was conducted.

2.10. Gas chromatographic and gas chromatographic–mass spectrometric analysis

Gas chromatographic analysis was carried out on a GC8000 gas chromatograph (Fisons Instruments, Wiesbaden, FRG) equipped with a 25 m × 0.25 mm i.d. × 0.25 μm film SE54 fused silica capillary column (CS Chromatographie Service, Langerwehe, FRG) and a flame ionization

Table 4

a. Bulk parameter and maceral composition of coal samples

Period	Series	Stage/ formation	Sample no.	Country	Location	Depth (m)	VRr (%)	Vitrinite (%)	Inertinite (%)	Liptinite (%)	TOC (%)	T_{max} (°C)	HI (mg/g)	OI (mg/g)
Permian														
	Upper Permian		CP1	Australia	Nipan o Seam, Bowen Basin		0.80	0.1	78.6		65.7	436	173	5
	Upper Permian		CP2	Australia	Upper Wynn, Sydney Basin		0.71	2.1	74.7		72.6	435	174	4
	Upper Permian		CP3	Australia	Bulli Seam, Sydney Basin		0.64				76.8	463	145	1
		Lower Zechstein	CP4	South China	Dahe Mine		0.64	63.5	15	12.5	76.1	440	312	8
	Rotliegend		CP5	Russia	Petchora Basin		1.08	83.5		16.5		454	196	9
		Artinskian/ Kungurian	CP6	Brasilia	Rio Benito Formation		0.44	58.6	12.2	1.8	31.6	424	120	17
		Artinskian/ Kungurian	CP7	Brasilia	Rio Benito Formation		0.43				32.6	429	136	15
	Lower Permian		CP8	Antarctica			0.41	63	14.5	17.5	62.4	420	33	79
Carboniferous														
	Westphalian	Westphalian D	CC1	Germany	Vertrauensflöz						68.2	421	271	12
		Westphalian C	CC2	England	Keekle 2194						54.7			
		Westphalian B	CC3	England	Potato Pot	24.7	0.80	25	57	11	74.6	432	255	8
		Westphalian B	CC4	England	Potato Pot	25.5	0.74	43.5	38	15	73.4	429	211	8
		Westphalian B	CC5	England	Potato Pot	29.5	0.79	41.5	36.5	19.5	74.7	433	255	8
		Westphalian B	CC6	England	Potato Pot	29.9	0.81	76.5	10	11	71.2	431	281	7
		Westphalian A	CC7	England	Rowland Gill	51.6	1.23	18.5	2.5		62.2	456	115	8
		Westphalian A	CC8	England	Potato Pot	59.6	0.85	71.5	14.5	8	68.2	433	245	8
		Westphalian A	CC9	England	Potato Pot	59.8	0.76				72.8	435	222,	9
		Westphalian A	CC10	England	Potato Pot	63.9	0.87	30	30.5	9	27.0	434	217	8
		Westphalian A	CC11	England	Potato Pot	77.9	0.82	73.5	10.5	14	77.9	435	239	7
		Westphalian A	CC12	England	Potato Pot	78.3	0.83	76.5	9	13	73.2	393	260	7
		Westphalian A	CC13	England	Distington I	12.9	0.81	51	25.5	14.5	73.0			
	Namurian		CC14	England	Dearham	45.1					45.8	437	286	9
	Namurian		CC15	England	Dearham	44.8	0.78	64	13.5	12.5	71.3	438	289	7
	Namurian		CC16	England	Dearham	55.3	0.77	39	2.5	15	71.8	438	240	8

	Namurian		CC17	England	Dearham	56.3					59.5	440	205	10
	Namurian		CC18	England	Rowland Gill	93.8	1.26				57.4	457	213	5
	Viséan		CC19	Russia	Moscow Basin		0.42		2.5	61.5	66.3	437	690	19
	Viséan		CC20	Russia	Moscow Basin		0.39	2	5	71.5	68.4	436	575	18
	Viséan		CC21	Russia	Moscow Basin		0.32	1.5	2.5	61.5	69.7	437	703	18
	Viséan		CC22	Germany	Borna Hainichen		0.57	65.5	19	13	58.1	430	153	18
	Viséan		CC23	Russia	Moscow Basin		0.41	28	17.5	29.5	50.8	416	258	37
	Viséan		CC24	Russia	Moscow Basin		0.37	66.5	10	14	54.6	412	150	44
	Lower Viséan		CC25	Spitsbergen	Mumien		0.88	37	28	31	81.5	438	256	7
Devonian														
	Upper Devonian	Givetium–Frasnium	CD1	Spitsbergen	Mimerdalen		0.76	22		77	67.2	440	496	5

b. Bulk parameter and maceral composition of fossils

Period	Series	Sample no.	Location	Origin	Flora realm	VRr (%)	Vitrinite (%)	Inertinite (%)	Liptinite (%)	TOC (%)	T_{max} (°C)	HI (mg/g)	OI (mg/g)
Permian													
	Lower Permian	FP1	Tansania	Glossopteris	Gondwana	0.45	30	44	15	65.2	417	43	38
Carboniferous													
	Upper Carboniferous	FC1	England	Coal Ball	Euramerian–cataysian	0.95	51	13	2	54.9	446	115	8
	Upper Carboniferous	FC2	England	Lepidodendron	Euramerian–cataysian	0.63	99			72.8	427	54	43
	Lower Carboniferous	FC3	Russia	Russian Platform	Euramerian–cataysian	0.36	25		64		428		
	Lower Carboniferous	FC4	Russia	Lepidodendron	Euramerian–cataysian	0.4	21	2	52				
	Lower Carboniferous	FC5	Russia	Lycopod-Spores	Euramerian–cataysian	0.42	35.5	10.5	52	65.4			
Devonian													
	Lower Devonian	FD1	Germany	Bad Münstereifel/ Brandschiefer	Euramerian (Psilophytaprovince)	1.14	42.5	1.5	8	29.6	437	105	14

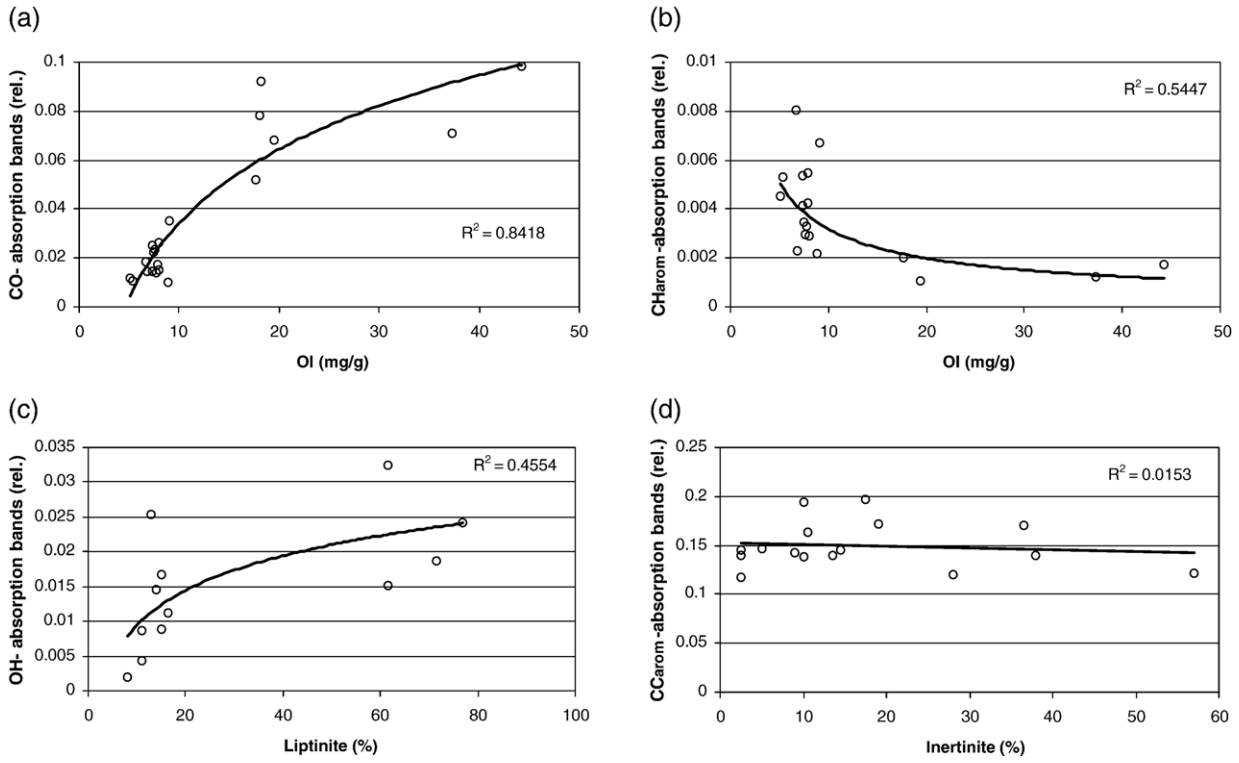

Fig. 4. Cross plots of normalized absorption bands *vs.* bulk parameters: CO_{arom}-absorption bands *vs.* OI (a), CH_{arom}-absorption bands *vs.* OI (b), OH-absorption bands *vs.* liptinite content (c), CC_{arom}-absorption bands *vs.* inertinite content (d).

detector (FID). Chromatographic conditions were: 1 µl split/splitless injection (injector temperature 270 °C) at 60 °C, splitless time 60 s, 3 min hold, then programmed at 3 °C/min to 300 °C, hydrogen carrier gas velocity was 35 cm/s.

GC–MS analyses were performed on a Finnigan MAT 8222 mass spectrometer (Finnigan, Bremen, FRG) linked to a HP5890 II gas chromatograph (Hewlett Packard, Palo Alto, USA) which was equipped with a 30 m × 0.25 mm i.d. × 0.25 µm film BPX5 fused silica capillary column (SGE, Weiterstadt, FRG). Chromatographic conditions were: 1 µl split/splitless injection (injector temperature 270 °C) at 60 °C, splitless time 60 s, 3 min hold, then programmed at 3 °C/min to 300 °C, helium carrier gas velocity was approx. 30 cm/s. The mass spectrometer was operated in a low resolution electron impact ionization mode (EI^+, 70 eV) with a source temperature of 200 °C scanning from 35 to 700 amu at a rate of 1 s/decade with an inter-scan time of 0.1 s.

Identification of individual compounds was based on comparison of EI^+-mass spectra with those of reference compounds, mass spectral data bases (NIST/EPA/NIH Mass Spectral Library NIST2000, Wiley/NBS Registry of Mass Spectral Data, 7th Ed., electronic versions) and gas chromatographic retention times, published elution patterns or retention indices.

Quantification of the identified compounds based on the integration of specific ion chromatograms. The areas determined were normalized to the internal standards for comparison of different samples. All compounds determined and the corresponding ion chromatograms used are summarized in Table 3.

3. Results

All results obtained for the coal samples will be presented according to the analytical methods applied. Generally, a correlation of chemical properties regarding the molecular structure of the non-extractable organic matter (obtained by chemical and pyrolytic degradation as well as FTIR spectroscopy) with the bulk parameter (TOC, Rock-Eval pyrolysis) and maceral composition was performed. In principal, correlations with a coefficient (R^2) above 0.5 were designated as significant, whereas trends with coefficients between 0.3 and 0.5 were characterized as minor correlations. R^2 values lower than 0.3 indicated no correlation.

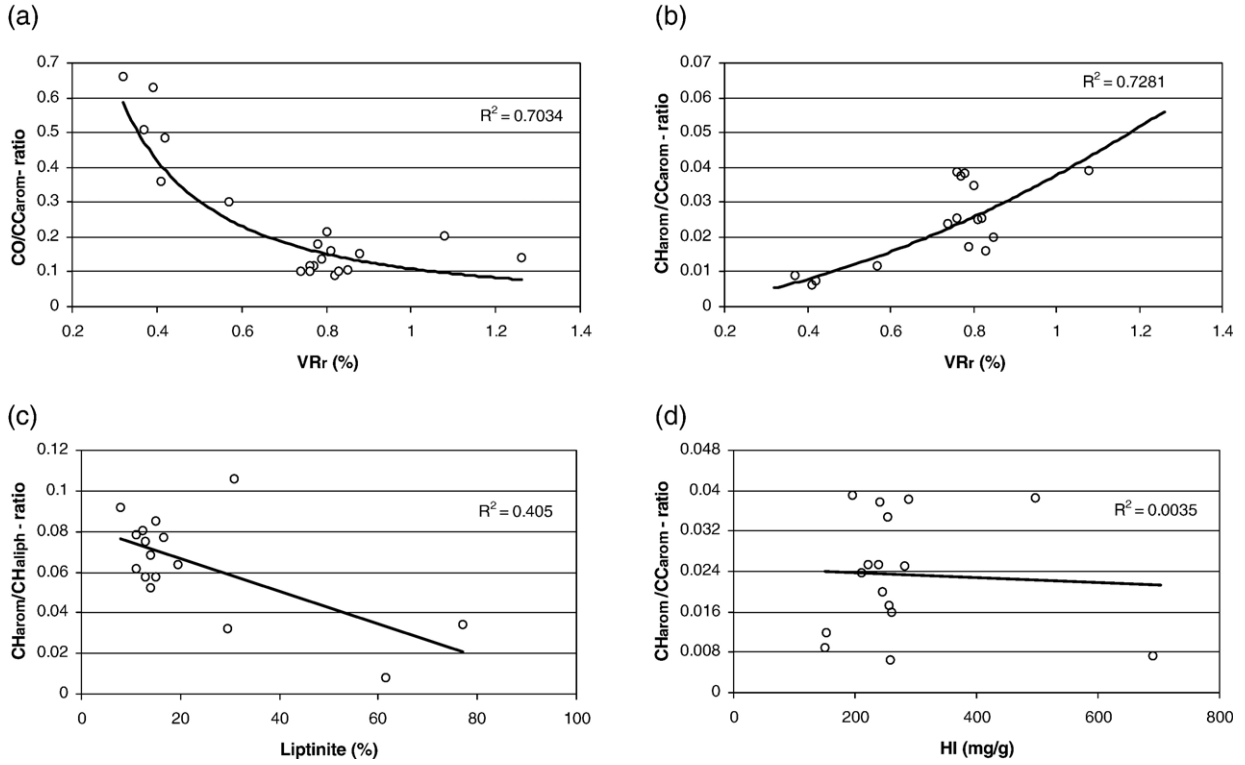

Fig. 5. Cross plots of different IR-band intensity ratios and bulk parameters: CO/CC_{arom} *vs.* VR_r (a), CH_{arom}/CC_{arom} *vs.* VR_r (b), CH_{arom}/CH_{aliph} *vs.* liptinite content (c), CH_{arom}/CC_{arom} *vs.* HI (d).

All data on bulk parameter and maceral composition are given in Table 4a+b.

3.1. FTIR spectroscopy

A set of 25 samples was measured by FTIR. Analysing the specific IR absorption bands of the organic matter allowed insights into the structural properties of the non-extractable organic residues. The principal attribution of absorption bands to individual functional groups within the organic matter is summarized in detail in Table 2 and based mainly on published data. Since the intensity of the signals depends not only on the relative proportion of the activated structure units but also on the type of functional group a direct comparison of signal intensity and concentration is not possible. However, an estimation of structural variations among the different samples was performed by integration of the individual signals and subsequent normalization to the total absorption of the IR spectra. Furthermore, variations were also found out by comparison of specific signal ratios as described in Table 2. Both IR parameter sets, calculated from single absorption bands as well as from specific IR-signal ratios, were subsequently correlated with bulk parameters (TOC, Rock-Eval-parameters, vitrinite reflectance, maceral composition) and sample age.

Numerous correlations of normalized absorption bands with bulk parameters exhibited significant trends ($R^2 > 0.5$). Some of these observations reflect similar chemical properties of the residues. For example the intensity of CH_{aliph}-absorption bands increased with higher HI values derived from the Rock-Eval pyrolysis. This is not surprising, because high HI-values reflect high amounts of aliphatic constituents. However, some correlations linked chemical parameters with information on the biogenic quality of the organic matter. The relative proportion of CH_{aliph}-absorption bands exhibited a negative trend with rising amounts of inertinite.

This correlation can be attributed to the fact that inertinite consists of more aromatic units instead of aliphatic chains (Taylor et al., 1998). A positive trend was observed with respect to CH_{aliph}-absorption bands and liptinite content. This can be explained by the composition of liptinite consisting dominantly of aliphatic-rich organic matter. With respect to coal type characterisation by Rock-Eval pyrolysis a significant positive trend was observed for CO-absorption bands with respect to the OI values (Fig. 4a), since a major part of organically bound

oxygen is associated to the group of carbonyl compounds (Hatcher and Clifford, 1997).

Beside the biogenic quality also thermal maturity and associated diagenesis affect the composition of the non-extractable organic matter. This fact was proven by rising proportions of CH_{arom}-absorption bands with increasing maturity, which is an indication for aromatisation processes during coalification (e.g. Hatcher et al., 1992). Additionally a significant negative correlation was observed for CO absorption bands with vitrinite reflectance. This can be attributed to the loss of oxygen containing functional groups during coalification.

A significant trend was also observed for the CH_{arom}-absorption bands, which decreased with rising OI content (Fig. 4b). Initially, a rise of CH_{arom}-absorption bands with higher OI values was predicted as the result of a preferred binding of oxygen to new formed aromatic structures during the coalification process (Ewbank et al., 1996; Hatcher and Clifford, 1997). However, maturity effects leading to defunctionalised organic matter and the resulting loss of oxygen seemed to be dominating the oxygen content.

Several correlations between individual absorption bands were revealed with minor significance ($0.3 < R^2 < 0.5$). A slight trend to decreasing CH_{aliph}-absorption bands with increasing proportions of vitrinite complemented the positive correlation obtained for CH_{aliph}-absorption bands and liptinite content as mentioned above. Also the positive trend of CH_{arom}-absorption with respect to T_{max} confirmed former observations regarding CH_{arom}-absorption bands and maturity.

Further weak correlations were observed for OH-absorption bands, which increased with higher liptinite content in the samples (Fig 4c). This trend reflects only the hydroxy-related composition of liptinite. Interestingly, also the oxygen-containing groups in liptinite can be dominantly attributed to the carbonyl groups of waxes (besides hydrogen-rich structures, Taylor et al., 1998), a similar trend was not observed for the CO bands. Only CC_{arom}-absorptions exhibited slight tendencies (to rise with increasing OI values, and to decrease with rising TOC content ($0.3 < R^2 < 0.5$).

Apart from the major and minor significant correlations discussed above most of the data deduced from the FT-IR analysis and compared with the bulk parameters exhibited no significant trends or tendencies ($R^2 < 0.3$). For some correlations between FTIR absorption bands and bulk parameters these observations were surprising. For example no correlation was obtained for CC_{arom}-absorption bands and inertinite (Fig. 4d) or CC_{arom}-absorption bands and vitrinite reflectance. For both relationships strong positive correlations were expected as the result of ongoing aromatisation with higher maturity or dominant proportion of aromatic organic matter in inertinite.

Furthermore, not only IR single absorption bands were analysed by comparison with bulk parameters but also specific absorption ratios reflecting characteristic changes in the chemical composition of the non-extractable organic matter. These correlations also revealed either significant, minor or not recognizable trends.

Chemical alterations related to maturity were indicated by significant trends ($R^2 > 0.5$) of CH_{arom}/CH_{aliph}-ratios as well as CO/CC_{arom}-ratios compared to the vitrinite reflectance. Increasing maturity went along with increasing CH_{arom}/CH_{aliph}-ratios as the result of ongoing aromatisation processes. Furthermore, the negative correlation of CO/CC_{arom}-ratios with vitrinite reflectance indicates defunctionalisation during coalification (see Fig. 5a). This trend correlates well with the maturity-related trend of normalized CO absorption bands described above.

However, for the CO/CC_{arom}-ratios further significant correlations were revealed. A negative trend of this ratio with rising vitrinite content corresponds to the fact that vitrinite is largely enriched in aromatic structures. Also, the reason for increasing CO/CC_{arom}-ratio with higher OI values is obvious.

Furthermore a decrease of the CH_{arom}/CC_{arom}-ratio values with increasing OI values was observed and indicates a decrease in oxygen content in highly mature coals characterized by large aromatic units (Hatcher et al., 1992). This assumption obviously supports the observation of decreasing CH_{arom}-absorption with increasing OI values as discussed before. However, this example illustrates the necessity for a very accurate view on the chemical information as revealed by the FTIR analyses. Both trends can be interpreted as the preferred association of organic oxygen with higher condensed aromatic structures in coals, leading to a decrease of hydrogen atoms attached to aromatic rings as compared to the proportion of aromatic carbon atoms (reflected by slightly increasing CC_{arom}-absorption). Hence, the insertion of oxygen (rising OI values) substitutes the hydrogen atoms attached to the aromatic systems and is accompanied by higher condensation of the carbon skeleton.

The positive correlation of the CH_{arom}/CC_{arom}-ratio with increasing maturity reflected by vitrinite reflectance values (Fig. 5b) is surprising at first. However, this correlation reflects a state of diagenetic transformation of the macromolecular organic matter that is characterized by beginning aromatisation without significant condensation. Therefore, especially the CH_{arom}-absorptions are affected by maturity (see also correlations of normalized CH_{arom}-bands and T_{max} as well as VR_r).

Table 5a
Trends revealed by individual IR spectroscopic absorption bands; +=significant positive trend ($R^2>0.5$), (+)=positive trend with minor significance ($R^2>0.3$), −=significant negative trend ($R^2>0.5$), (−)=negative trend with minor significance ($R^2>0.3$)

	VRr (%)	Vitrinite (%)	Inertinite (%)	Liptinite (%)	TOC (%)	T_{max} (°C)	HI (mg/g)	OI (mg/g)
CH_{aliph}		(−)	−	+	(+)			
CH_{arom}	+					(+)		−
CC_{arom}					(−)			(+)
OH				(+)				
CO	−							+

Slight, but recognizable trends ($0.3<R^2<0.5$) were observed for the CH_{arom}/CH_{aliph}-ratios. With higher proportions of liptinite in the samples this ratio decreased (Fig. 5c). As pointed out above, liptinite features many aliphatic structural moieties and, consequently, this observation correlates with the corresponding positive trend for normalized CH_{aliph}-absorption bands. Also the negative correlation of CH_{arom}/CH_{aliph}- and HI values represents the more aliphatic properties of hydrogen-rich organic matter.

Furthermore, the CO/CC_{arom}-ratios exhibited two slightly positive tendencies. They increased with higher proportions of liptinite and increasing HI values. Hence, as pointed out before rising proportions of liptinite contents affected not only the hydrogen-but also the oxygen-content as compared to aromatic structures. A rising trend was also observed for the OH/CC_{arom}-ratios with increasing liptinite content.

However, the major part of specific absorption ratios revealed no observable trends with respect to the bulk parameters. An example is illustrated in Fig. 5d. All correlations of individual (normalized) IR spectroscopic absorption (Table 5a) as well as of specific absorption ratios are summarized in Table 5b with respect to their significance.

3.2. Pyrolysis

In total 33 samples were determined by Curie point pyrolysis directly linked to GC/MS (see Table 1). These analyses were carried out on the pre-extracted samples either without any further treatment or in combination with TMAH in order to enhance the pyrolytic cleavages and to convert polar carboxylic acids to the corresponding methyl esters.

Qualitative analysis revealed numerous individual compounds belonging to the compound classes of aliphatic and aromatic hydrocarbons, polycyclic aromatics, carboxylic acids and further oxygen-containing substances (phenols, dibenzofurane). The pyrolytic signature varied significantly for the samples investigated. On the one hand aliphatic rich samples occurred as illustrated in Fig. 6a. On the other hand for numerous samples aromatic compounds were the dominant pyrolysis products (see Fig. 6b).

All compounds considered for the quantitative analyses are summarized in Table 3 (see experimental section). The pyrolytic yields of these specific compounds were used to compare the quantitative distribution with the parameters reflecting bulk chemical properties (HI, OI, TOC), the biogenic sources (maceral composition) and maturity (VR_r, T_{max}). These correlations were performed in the same way as presented for the FTIR spectroscopic results.

Despite of this considerable amount of data received by Curie-point pyrolysis, only few trends were observed with a major significance. Correlations with minor significance were more frequently detected, but the major part of correlations exhibited no tendencies. These observations are summarized in Table 6a.

In detail, only a few comparisons exhibited a significant correlation. A clear dependency of increasing OI-values with higher phenol and fatty acids content was

Table 5b
Trends revealed by ratios between specific absorption bands; +=significant positive trend ($R^2>0.5$), (+)=positive trend with minor significance ($R^2>0.3$), −=significant negative trend ($R^2>0.5$), (−)=negative trend with minor significance ($R^2>0.3$)

	VRr (%)	Vitrinite (%)	Inertinite (%)	Liptinite (%)	TOC (%)	T_{max} (°C)	HI (mg/g)	OI (mg/g)
CH_{arom}/CH_{aliph}	+			(−)			(−)	
CH_{arom}	−	−		(+)				+
OH/CC_{arom}				(+)			(+)	
CH_{arom}/CC_{arom}	+				(+)	(+)		−

observed characterizing both functional groups as major oxygen containing structural units in the macromolecular organic matter. Furthermore, a negative trend of HI values with increasing alkylbenzene content indicated the effect of aromatic groups on the hydrogen atom balance (see Fig. 7). An astonishing trend was the

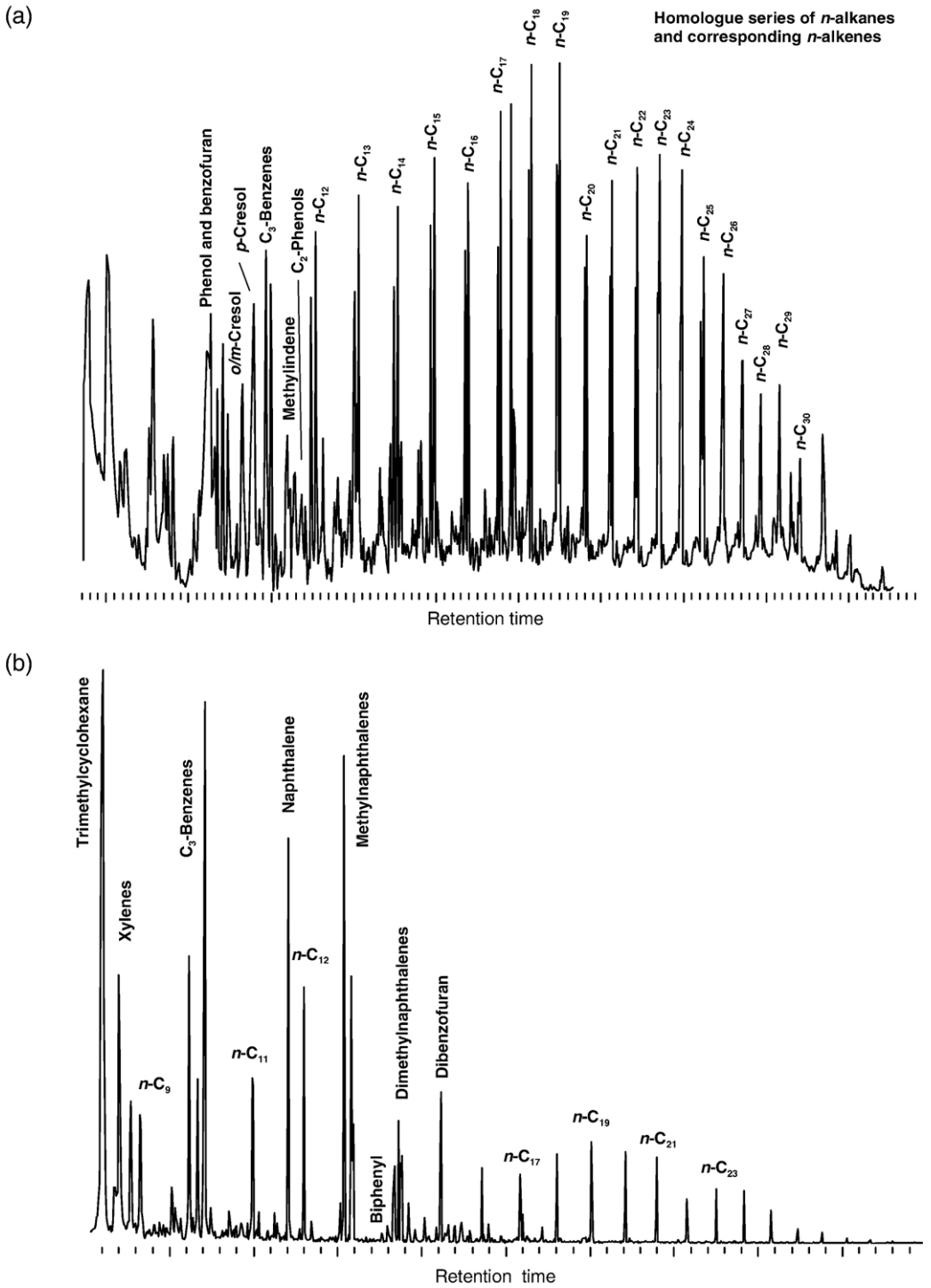

Fig. 6. a: Exemplary pyrogram of an aliphatic dominated lepidodedron from the Moscow Basin (sample FC4). b: Exemplary pyrogram of an aromatic dominated coal sample from Spitsbergen (sample CC25).

Table 6a
Trends of indiavidual substances revealed by pyrolysis; +=significant positive trend ($R^2>0.5$), (+)=positive trend with minor significance ($R^2>0.3$), −=significant negative trend ($R^2>0.5$), (−)=negative trend with minor significance ($R^2>0.3$)

	VRr (%)	Vitrinite (%)	Inertinite (%)	Liptinite (%)	TOC (%)	T_{max} (°C)	HI (mg/g)	OI (mg/g)
n-alkanes				(+)	(−)			
n-alkenes								
n-alkines	(+)					+		
Acenaphthylene		(+)		(−)				
Acenaphthene								(+)
Fluorene								
Phenanthrene/anthracene							(−)	
Methylphenanthrenes	(+)			(−)			(−)	
Fluoranthene/pyrene								
Methylpyrenes								
Phenol								+
Methylphenols								
C_2-phenols			(+)					
Dibenzofuran								
Methylbenzenes							−	(+)
C_2-benzenes							(−)	
C_3-benzenes		(+)					(−)	
Fatty acids							(−)	+

positive correlation of *n*-alkine contents and T_{max}, but it has to be considered that only little data existed in this case.

Most of the correlations were of minor statistical significance ($0.3<R^2<0.5$). The trends of increasing content of several aromatic compounds (alkylated benzenes, phenanthrene/anthracene and methylated homologues) with decreasing HI-values support the observations described for alkylbenzenes.

However, several trends were observed concerning the maceral composition. In liptinite-rich samples less aromatic but more aliphatic units were present as indicated by the contents of *n*-alkanes, acenaphthylene and methylphenanthrenes in the pyrolysis products. On the contrary, higher abundances of vitrinite and inertinite correlated with higher pyrolytic yields of acenaphtylene, C_3-benzenes and alkylphenols, respectively, confirming the higher content of aromatic structures in these maceral groups (Hatcher et al., 1992; Taylor et al., 1998).

In order to get a more general and clearer view on the chemical properties and alterations of the macromolecular organic matter as revealed by pyrolysis all substances with similar chemical structures were combined to compound groups. The correlations of the compounds in question were proved to be consistent as illustrated exemplarily for alkylated benzenes and *n*-alkanes/alkenes in Fig. 8. In addition, chemical aspects and known biogenic or diagenetic interrelationships were considered.

This evaluation revealed several compound groups combining different substances with the same behaviour in terms of occurrence and pyrolytic yield. Results are presented in Table 6b and include the groups of aliphatics (Aliph), alkylbenzenes (Benz), polycyclic aromatic hydrocarbons (PAH), and oxygen containing substances (Oxyg). Both alkylbenzenes and polyaromatic compounds were additionally combined to the group of aromatics (Arom). The pyrolytic yields of all compounds belonging to the same compound group were combined and based on these values specific group ratios were generated reflecting principal alterations in the non-extractable organic matter of the coal samples investigated.

Most of these correlations did not exhibit any significant tendency in particular with respect to the thermal maturity (VR_r, T_{max}) and TOC values. However, several correlations of minor significance support information on the quality of the primary composition of the precursor plant material. The Aliph/Arom ratio exhibits a significant positive correlation with higher HI-values and, furthermore, negative tendencies with higher content of vitrinite as well as with higher content of inertinite. Also a positive

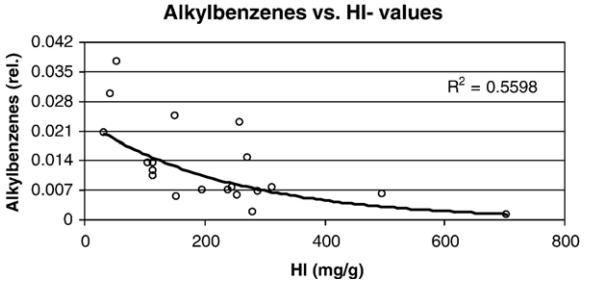

Fig. 7. Correlation between alkylbenzenes and HI values.

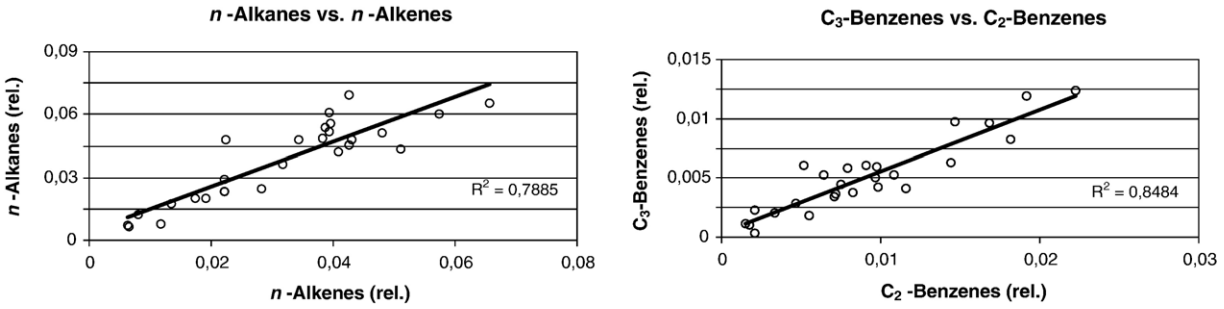

Fig. 8. Cross plots of similar chemical structures.

trend with increasing amounts of liptinite is recognisable. Likewise, for the Oxyg/Aliph ratio slight positive trends with both vitrinite and inertinite were observed. All these correlations illustrate the higher amount of oxygen in vitrinite and inertinite rich samples in contrast to higher aliphatic content in liptinite and hence are not surprising (van Krevelen, 1993; Taylor et al., 1998).

3.3. TMAH-thermochemolysis

Besides pyrolysis also an approach combining thermal and chemical techniques was used to identify specific degradation products of the non-extractable organic matter of the coal samples investigated. This thermochemolytic technique assisted by tetramethylammonium hydroxide (TMAH) was established by Caallinor (1989). Since that time TMAH-thermochemolysis has been frequently applied to characterize different kinds of macromolecular biomolecules and their diagenesis products, e.g. lignin (McKinney et al., 1995; Filley et al., 1999), degraded wood (Hatcher et al., 1995; del Rio et al., 1998) or soil humic acids (Ikeya et al., 2004).

TMAH-thermochemolysis was applied on 28 coal samples. Noteworthy, benzoic and fatty acids were found to be dominant compounds. These compounds were frequently characterized as main products generated by TMAH-thermochemolysis of plant material or plant related samples (Hatcher and Clifford, 1994; Martin et al., 1995; del Rio and Hatcher, 1998). Furthermore, these compounds provided the major part of notable correlations as revealed by TMAH-thermochemolysis. Besides the main products, aromatic acids and hydrocarbons, which represent a minor proportion of the thermochemolysis products, were included into the analysis. Chemically similar substances of the macromolecular matter were combined comprising aliphatic and aromatic hydrocarbons and selected oxygen containing aromatics.

Significant trends ($R^2>0.5$) were observed for the relative content of methoxymethylbenzoic acids. These compounds were less abundant with increasing maturity (VR_r, T_{max}; see Fig. 9a) as a consequence of defunctionalisation during coalification. Additionally, the amount of methoxymethylbenzoic acids was reduced in samples characterized by higher HI values (Fig. 9b), whereas higher OI values led to rising amounts of these aromatic acids. With respect to the fatty acids a lower relative content of fatty acids correlated with higher HI values and to a minor extent with lower OI values.

For the maceral composition only minor tendencies were observed in particular for inertinite and liptinite. Inertinite rich samples were characterized by lower contents of benzoic acid and methylated homologues after thermochemolysis, whereas vitrinite rich samples exhibited higher amounts of benzoic acid.

For all other substances only very few correlations were observed supporting no further relevant information

Table 6b
Trends of ratios between compound classes revealed by pyrolysis; +=significant positive trend ($R^2>0.5$), (+)=positive trend with minor significance ($R^2>0.3$), −=significant negative trend ($R^2>0.5$), (−)=negative trend with minor significance ($R^2>0.3$)

	VRr (%)	Vitrinite (%)	Inertinite (%)	Liptinite (%)	TOC (%)	T_{max} (°C)	HI (mg/g)	OI (mg/g)
Aliph/Arom		(−)	(−)	(+)			+	
Oxyg/Aliph		(+)	(+)					
Oxyg/Arom								
Oxyg/Benz								
Oxyg/PAH_s								
Oxyg/Aliph+Arom		(+)						(+)

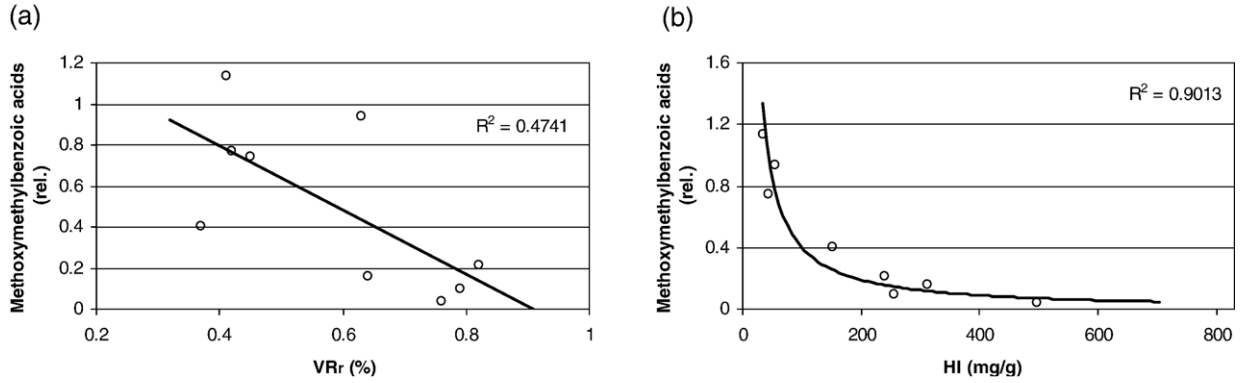

Fig. 9. Methoxymethylbenzoic acids correlated with VR_r (a) and HI values (b).

(Table 7a). Also the statistical analysis of compound group ratios revealed no significant or notable results (see Table 7b).

3.4. Chemical degradation

The chemical degradation procedures applied to the coal samples in a sequential mode comprised alkaline hydrolysis, boron tribromide treatment and ruthenium tetroxide oxidation. Although chemical degradation procedures are generally time consuming, these techniques were applied to reveal some more detailed structural information on the macromolecular organic matter.

Principally, it has to be noted that chemical degradation of non-extractable organic matter released two different pools of compounds. The first one comprises compounds formerly covalently bound and released specifically by the degradation reaction initiated. On the other hand, such alterations of the macromolecular carbon backbone also affect the weaker bound compounds. Hence, a second group of formerly non-covalent bound compounds were detected, additionally.

The results will be discussed with a special focus on the structural properties of the degradation products considering the specific degradation reactions. This structural information complemented the results obtained by FTIR spectroscopy and pyrolysis.

Table 7a
Trends of individual substances revealed by TMAH-thermochemolysis; +=significant positive trend ($R^2>0.5$), (+)=positive trend with minor significance ($R^2>0.3$), −=significant negative trend ($R^2>0.5$), (−) = negative trend with minor significance ($R^2>0.3$)

	VRr (%)	Vitrinite (%)	Inertinite (%)	Liptinite (%)	TOC (%)	T_{max} (°C)	HI (mg/g)	OI (mg/g)
n-alkanes							(+)	(−)
n-Alkenes								
n-alkines								
Acenaphthylene								
Acenaphthene								
Fluorene								
Phenanthrene/anthracene								
Methylphenanthrenes								(−)
Fluoranthene/Pyrene								
Methylpyrenes								
Phenol								
Methylphenols								
C_2-phenols								
Dibenzofuran								
Methylbenzenes								
C_2-benzenes								
C_3-benzenes								
Benzoic acid			(−)	(+)				
Methylbenzoic acids			(−)					
Methoxybenzoic acids								
Methoxymethylbenzoic acids	−					(−)	−	+
Fatty acids						(−)	−	(+)

Table 7b
Trends of ratios between compound classes revealed by TMAH-thermochemolysis; +=significant positive trend ($R^2>0.5$), (+)=positive trend with minor significance ($R^2>0.3$), −=significant negative trend ($R^2>0.5$), (−)=negative trend with minor significance ($R^2>0.3$)

	VRr (%)	Vitrinite (%)	Inertinite (%)	Liptinite (%)	TOC (%)	T_{max} (°C)	HI (mg/g)	OI (mg/g)
Aliph/Arom	(+)		(−)					
Oxyg/Aliph								
Oxyg/Arom						(−)		
Oxyg/Benz								
Oxyg/PAH_s								
Oxyg/Aliph+Arom								

3.4.1. Alkaline hydrolysis

Alkaline hydrolysis was applied to cleave ester bonds within the macromolecular matter and to release ester bound moieties of low molecular weight from the macromolecular carbon backbone. Hence, dominantly fatty acids, aromatic acids and phenols were detected.

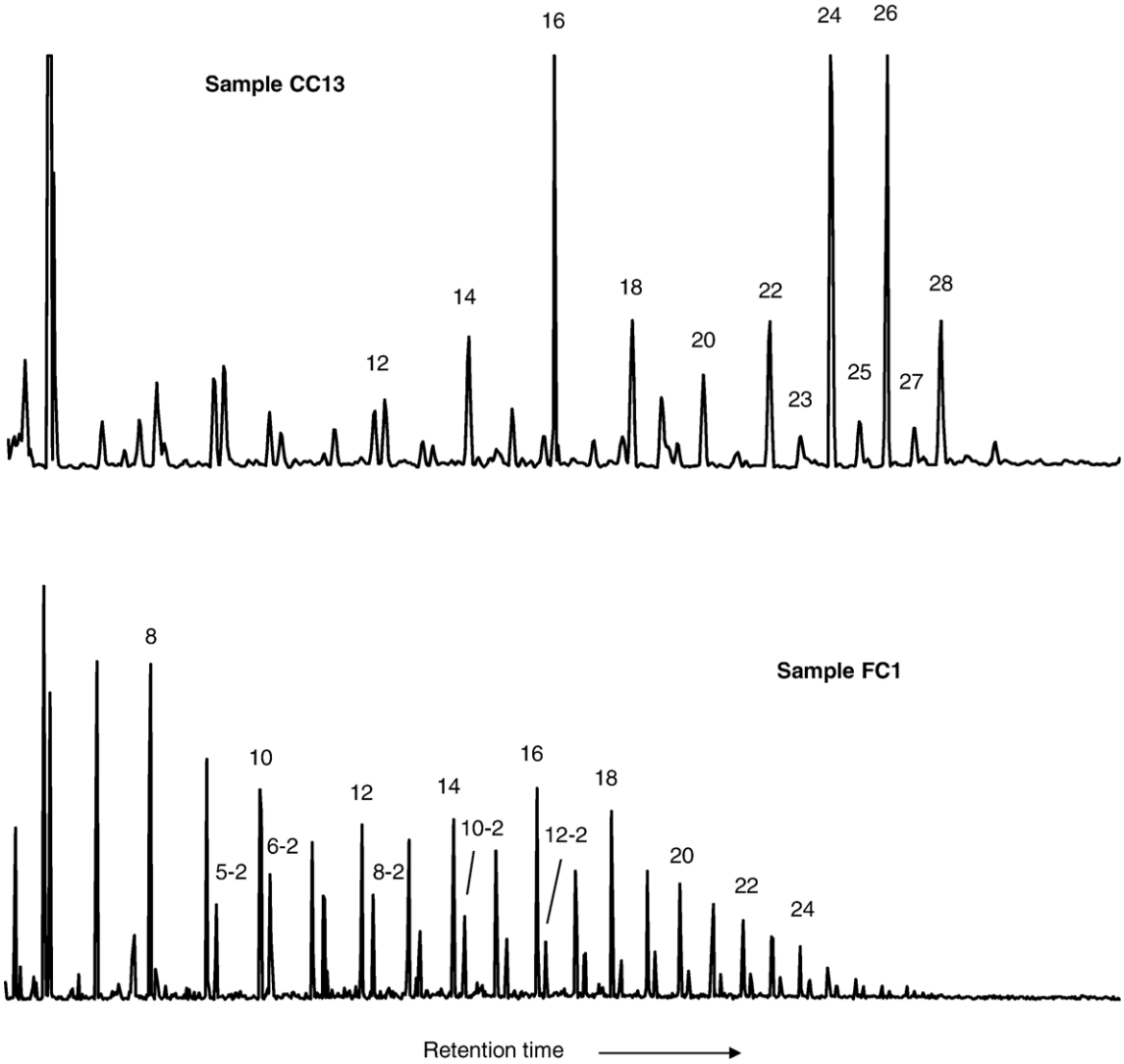

Fig. 10. Distribution pattern of fatty acids in coals (sample CC13) and fossils (sample FC1), *m/z* 74 (Numbers represent carbon numbers of carboxylic acids, numbers added with "−2" represent carbon numbers of dicarboxylic acids. All compounds were detected as methyl esters.

Table 8
Qualitative results of BBr_3-treatment analysis (++=high concentrations, +=minor concentrations, o=traces)

Samples	Dominant maceralgroup	Aliphatics		Brominated aliphatics		Phenols		Acids				
		Alkanes	Alkenes	Brominated *n*-alkanes	Brominated C_5/C_6-aliphatics	Methyl-phenols	Dimethyl-phenols	Benzoic acid	Methyl-benzoic acid	Methoxy-benzoic acid	Methoxy-methy-benzoic acids	Fatty acids
Coals:												
CP4	v	o		o	++	+	++					
CP7	v	+			+	+	++					
CP8	v	++	+		++	+	++	o	+	o	o	
CC2		++			++		o	o	o			
CC3	i	+		o	+	+	++	o				
CC4	v,i	+			+							
CC5	v,i				++	+	++	o	o	o	o	o
CC6	v			+	+							
CC8	v	+			++	++	++	+	+	+	+	
CC9		++		+	++							
CC10	v,i	++	+	+	++							
CC11	v	++	o	+	+	+	++	o				o
CC12	v	+			++							
CC13	v,(i)				++							++
CC14					++							
CC15	v				++	o	o	o	o	o	o	o
CC16	v	++			++	o	+	+	o	o		
CC21	l				++	+	++	o	o	o	o	
CC23	l,v,(i)	+		o	++	+	++	o	+	o	o	
CC24	v			o	++	++	++					o
CD1	l	++	++		+	+	++		o	o	o	
Fossils:												
FP1	v,i	+		+	++	+	++					+
FC2	v			+	++	+	++	o	+	o	+	
FC3	l				++	+	++	o	+	o	+	
FC4	l	o		o	++	+	+					o
FC5	l,(v)				++	++	++	o		o	o	
FD1	v	++		+	++	+	++		+	+	+	

Interestingly, aliphatic alcohols were not identified. Additionally, a second group of compounds, which were formerly only occluded but not covalently bound, comprised *n*-alkanes, polycyclic aromatic compounds (dominantly acenaphthene, phenanthrene, anthracene, fluoranthene, pyrene and its alkylated homologues) and dibenzofuran. Alkylated benzenes were rarely detected. Comparing the yields of individual compound groups revealed by alkaline hydrolysis, very similar relative amounts were observed with respect to both the coal and the fossil samples. This observation considered the phenols, benzoic acids and PAHs.

On the contrary, fatty acids were detected in higher amounts in the fossils as compared to the coal samples. Noteworthy, the pattern of fatty acids differed significantly in both coal and fossil samples as illustrated in Fig. 10. Coal derived fatty acids exhibited distribution maxima at hexadecanoic acid (palmitic acid) as well as tetracosanoic and hexacosanoic acids with a strong even–odd predominance. The pattern of fossil derived fatty acids were characterized dominantly by an equalized distribution with respect to odd and even numbered members and maximum concentrations of short chain carboxylic acids (*n*-C_7 to *n*-C_9). This distribution is superimposed by slightly enhanced concentrations of hexadecanoic and octadecanoic acid. Beside the carboxylic acids also dicarboxylic acids were detected in high concentrations. All differences within the patterns suggested two different sources of fatty acids in the coal and fossil samples investigated. The dominance of *n*-C_{16} and *n*-C_{24} to *n*-C_{28} acids with a strong even-over-odd predominance is a very well known distribution of low molecular weight lipid components in terrestrial land plant, especially in cuticular waxes or biopolesters (e.g. cutin or suberin). On the contrary the elevated amounts of short chain components without any predominance

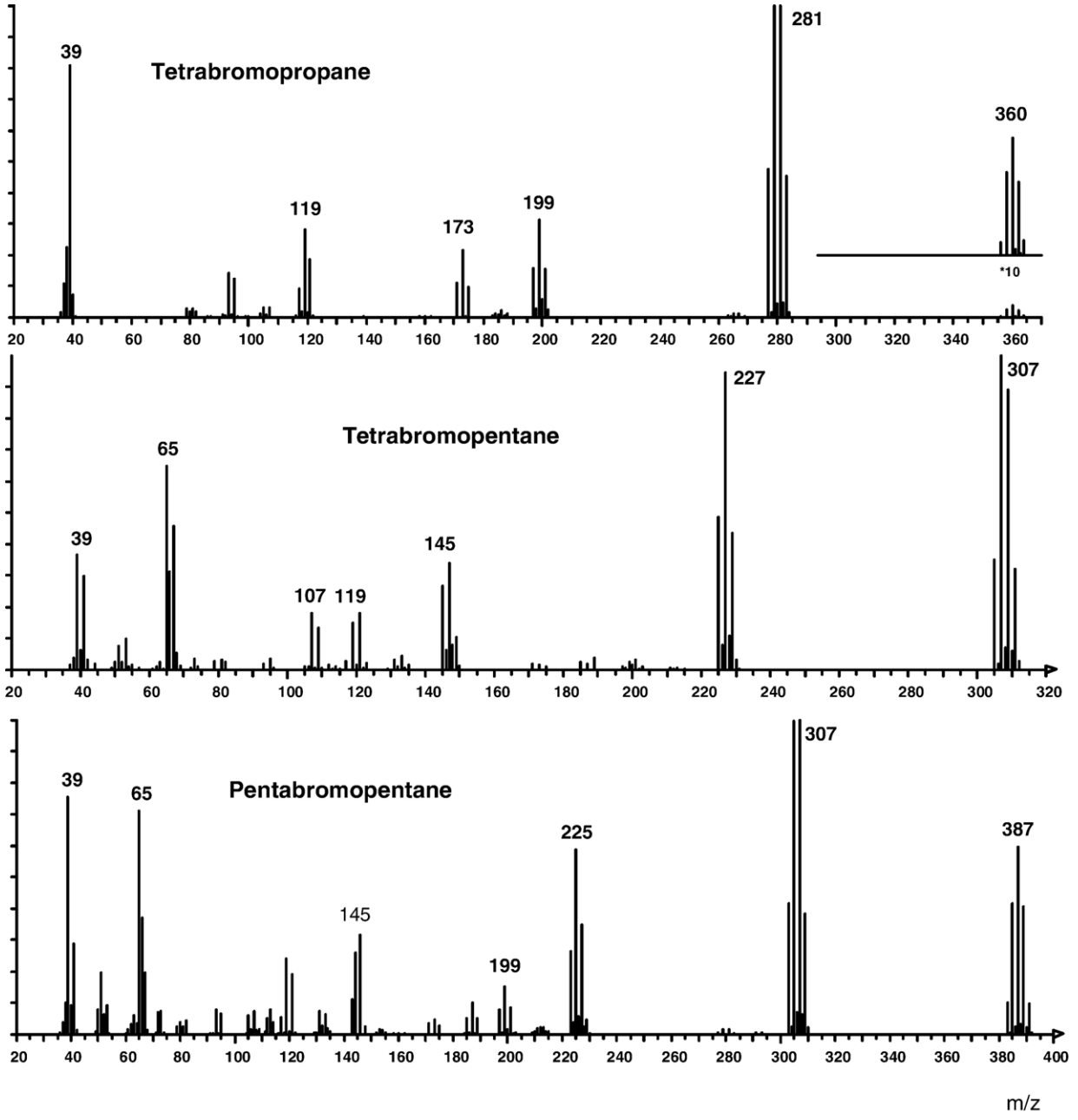

Fig. 11. Distribution pattern of tetra- and pentabrominated short chain aliphatics.

contradict an acetate based chain elongation as known for the above mentioned fatty acids. The appearance of this unusual pattern may be related to much stronger degradation due to weathering and oxidation of the fossils as compared to the coals. The contemporary occurrence of dicarboxylic acids suggests the degradation of polyester based biomacromolecules. However, a distinct association to specific plant organs or functions cannot be performed and the information extractable from fatty acid distributions in fossil samples are very limited so far.

Furthermore, compounds detected in the coal samples after alkaline hydrolyses did not contribute significantly to the macromolecular structures, because the hydrolysis products are not correlated with the carbon backbone of the non-extractable residues. Therefore, all results obtained by alkaline hydrolysis are regarded to be of minor significance for this study.

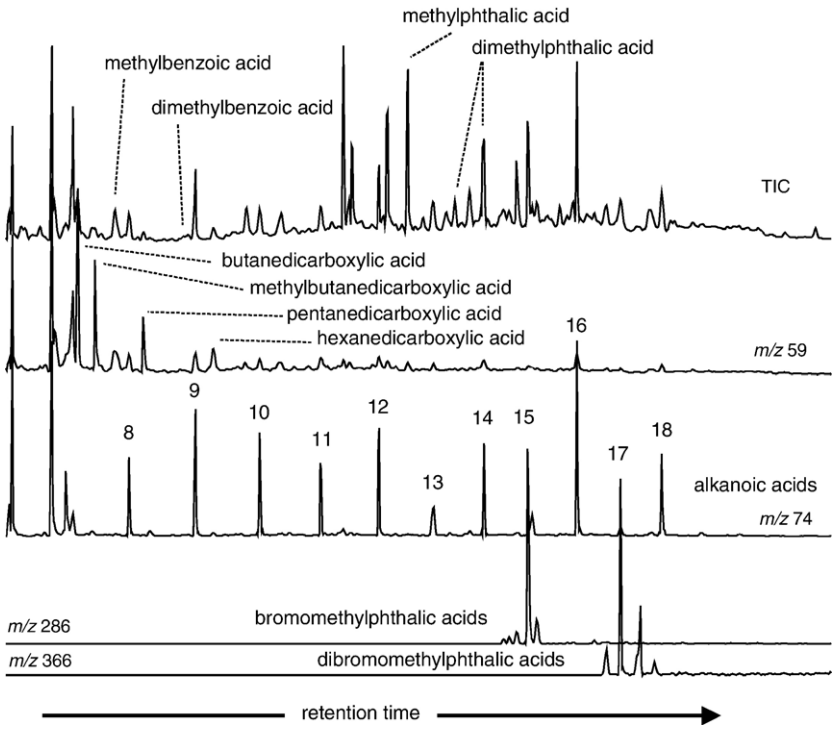

Fig. 12. Different ion traces displaying degradation products of RuO_4-oxidation.

3.4.2. Boron tribromide treatment

Boron tribromide (BBr_3) is a strong Lewis acid and, therefore, a suitable reagent to initiate ether and ester bond cleavages in macromolecular organic matter (Ping'an Peng et al., 1997). According to earlier studies (Jenisch et al., 1990; Vella and Holzer, 1990) the spectra of boron tribromide degradation products predominantly consist of alcohols and brominated aliphatics as the result of ether bond cleavage, as well as of carboxylic acids and alcohols produced by ester bond cleavages. Minor by-products were *n*-alkenes and fatty acids. Although the sequential application of the degradation methods as applied in this investigation should allow to focus mainly on the ether derived products of the BBr_3 treatment, also formerly ester bonded products were detected.

Main products were attributed to the group of phenols and substituted benzoic acids (see Table 8) representing ester or ether linked benzoyl/phenolic moieties with methyl and methoxy substitution. These moieties are structurally related to lignin derived macromolecules, but did not match exactly the structural properties, because lignin consists dominantly of phenylpropyl units. Correlation with the maceral composition indicated a preferential association of the aromatic carboxylic acids and phenols with vitrinite. In inertinite rich samples no or only minor concentrations were observed. Degradation of vitrinite rich samples released only some of these compounds, whereas each liptinite dominated sample released both benzoic acids and phenols after BBr_3 treatment. Since liptinite is not predominantly derived from woody material, a primary lignin binding for these compounds cannot be assumed. A second very specific group of BBr_3 treatment products were mono- and dibrominated long chain alkanes (approx. C_{10} to C_{20}). Considering the reaction process these products indicate the covalent incorporation of long chain aliphatic moieties linked via one or two ether bridges. Such structural units are proposed to be components of land plant biopolymers e.g. cutin. Additionally, a huge amount of tetra- and pentabrominated short chain aliphatics with three to five carbon atoms were tentatively identified. Characteristic mass spectra are presented in Fig. 11. Following the argumentation stated for low brominated aliphatics, the occurrence of these compounds has to be attributed to propyl to pentyl moieties with a maximum of four to five ether bridges to the macromolecular matter. Considering a possible transormation of hydroxy groups to bromine substituents during the BBr_3 treatment, also less ether bridges but hydroxy groups attached to the cyclic aliphatics can be assumed to be part of the macromolecular organic matter investigated.

Interestingly, high concentrations of *n*-alkanes were also observed, although these compounds are not specific products of BBr_3 treatment. The concentrations detected were in the same range as those of the other BBr_3 treatment products discussed above. However, further obviously

non-covalent bound components were not observed. The relative amounts of the different compound groups were in the following order:

Polybrominated short chain aliphatics, phenols > *n*-alkanes > mono- to dibrominated long chain alkanes, substituted benzoic acids, fatty acids.

3.4.3. RuO_4-oxidation

The oxidation of the non-extractable residues by RuO_4 is the strongest degradation method applied in this study. This oxidation attacks the carbon backbone especially of alkylaromatic and polycyclic aromatic moieties generating aliphatic carboxylic acids and substituted benzene carboxylic acids, respectively (Stock and Wang, 1985; Choi et al., 1988; Boucher et al., 1991).

In several samples these specific degradation products were observed as illustrated in Fig. 12. In detail alkylated phthalic and benzoic acids as well as mono- and dicarboxylic aliphatic acids were identified. The distributions of the aliphatic monocarboxlic acids reflect structural differences of the aliphatic moieties. On the one hand, a dominance of hexadecanoic and octadecanoic acids was observed with an even–odd predominance. On the other hand, a uniform pattern was observed for carboxylic acids in the range between C_6 and C_{18} (see Fig. 12).

To a minor extent oxygenated and hydroxylated carboxylic acids appeared. Furthermore, formerly non-covalent bound substances were released belonging to the *n*-alkanes, alkylated benzenes and phenols.

Interestingly, also brominated compounds were detected, representing structural units within the macromolecules, that were transformed by the BBr_3 treatment, e.g. by cleavage of intramolecular ether bridges, but were not released as low molecular weight compounds. The combination of both degradation techniques allowed a more detailed insight into the structural subunits of the macromolecular organic matter. For example the bromomethylphthalic acids indicated polycyclic aromatic units cross linked via an ether bond.

In summary, the high amount of aliphatic carboxylic acids reflects very well the aliphatic moieties within the carbon backbone. Additionally, significant proportions of aromatic moieties were identified in nearly all samples. However, for several samples the oxidation yield was very low, maybe as a result of the other degradation procedures formerly applied.

4. Discussion

Comprehensive chemical analyses as well as microscopical investigations were performed in order to provide information on the quality of the biogenic input, the diagenetic changes or evolutionary trends. The results obtained from the different analyses allowed insights into different pools or fractions of the non-extractable organic matter depending on the analytical method applied. However, for numerous samples different analytical results revealed similar chemical information. In particular the differentiation of aliphatic and aromatic rich material as well as the characterisation of oxygen containing moieties was evident by results of complementary analytical methods. For example increasing amounts of aliphatic products released by pyrolysis correlated very well with increasing intensities of CH_{aliph}-bands in FTIR spectra or with elevated concentrations of fatty acids or brominated alkanes detected after RuO_4 oxidation or BBr_3 treatment, respectively. Consequently, positive correlations of petrographical and bulk parameters with chemical information by different analytical methods were often obtained. This was especially evident for maturity and maceral composition trends, which will be discussed in the following chapter in more detail. However, it has to be noted that numerous trends were only observed for results derived from just one analytical method. This fact demonstrates the necessity to apply several complementary analytical tools in order to obtain more comprehensive information on the chemical and petrographical properties of coal material.

4.1. Primary composition of the precursor plant material and diagenetic processes

It is well known that the quality of the biogenic matter influences the composition of its diagenesis products in coals. However, coals represent a mixture of plant material deposited over an extended period of time and derived from different plant types ranging from higher land plants to fresh water algae and bacteria. Furthermore, different parts or organs of plants resist differently over geological time periods. For the macromolecular organic matter several types of compounds are known to survive more or less altered. These groups of geopolymers include dominantly compounds derived from lignin, cutin, suberin and sporopollenin. They represent different types of plant material namely wood, cuticles, roots and spores. This more resistant organic matter and its associated macromolecular constituents can be differentiated by microscopical analyses revealing the maceral group composition.

The coal samples investigated covered a wide range of maceral compositions (see Fig 13).

However, chemical composition and maceral characteristics correlate only to a minor extent and dominantly with trends only but not significant correlations. Generally,

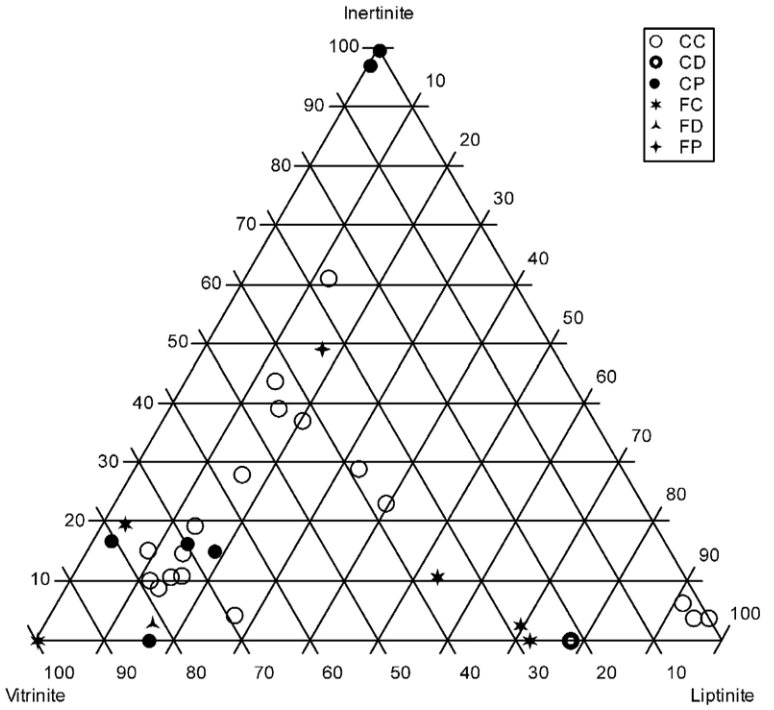

Fig. 13. Maceral group distribution; CC=coal Carboniferous; CD=coal Devonian; CP=coal Permian; FC=fossil Carboniferous; FD=fossil Devonian; FP=fossil Permian.

contrary trends were observed for liptinite and vitrinite/inertinite in most of the correlations or trends observed. For example increasing CH_{alip}-IR-bands were detected either for increasing liptinite content or decreasing vitrinite/inertinite content. The same trends were evident for the Aliph/Arom ratio derived from pyrolytical analysis correlated with the maceral composition. These observations contrast significantly liptinite from the other macerals from a chemical point of view. Similar conclusion have been formerly reported (Choi et al., 1988; Hatcher, 1990; Stankiewicz et al., 1996; Mastalerz et al., 1998; Ward and Gurba, 1999).

However, there are several samples with a distinct enrichment of individual macerals reflecting enhanced concentration of selected plant material. Especially for these groups a very good correlation of chemical composition and petrographic characterisation was observed finding out the characteristics of individual plant parts. A first group covered three samples of the Moscow Basin (CC19–CC21) with liptinite rich organic matter (61.5 to 71.5%) which are characterized as Cannel-Boghead-coals. More detailed petrographical analyses revealed alginite and sporinite as the main macerals with only minor contributions of cutinite.

Hence, the liptinite at low maturity is chemically characterised by high amounts of aliphatic moieties representing the alginite and sporinite contribution or, accordingly, the corresponding organic macromolecules algenan and sporopollenin, respectively. These constituents resulted in high amounts of *n*-alkanes released by pyrolysis, high absorption intensities of aliphatic CH-bands in FTIR analysis and elevated amounts of fatty acids obtained after RuO_4 oxidation. Further evidence of minor degree was observed for the contribution of sporopollenin, a biogenic macromolecule (Wiemann et al., 2001) corresponding with the maceral sporinite. This includes elevated OH-bands (FTIR analysis) and high amounts of phenols released by pyrolysis. The lack of aromatic moieties in the samples CC19 to CC21 was obvious as illustrated by low aromatic C–H vibration bands, low concentrations of aromatic carboxylic acids released via RuO_4 oxidation and only minor amounts of aromatic compounds derived from pyrolysis degradation.

These comprehensive analytical observations agree very well with results formerly published for sporinite, algenan or liptinite-rich samples (Largeau et al., 1986; Choi et al., 1988; Hayatsu et al., 1988). However, it has to be noted, that all these studies used one or at most two different analytical techniques to characterize the macromolecular organic matter. A comprehensive view by different but complementary analytical techniques has been published rarely.

A second group of specific samples were characterised as vitrinite rich coals and fossils. This group comprises several coal samples from the Potato Pot bore hole (vitrinite content at or above 70%), a coal sample derived from the Moscow Basin (CC24, vitrinite content: 66.5%) and one Lepidodendron fossil sample (FC2, vitrinite content: 99%). All samples were chemically characterized by mono- and polyaromatic compounds dominating the pyrolyzates, high intensities of the CH_{arom} IR-absorptions and elevated concentrations of aromatic acids in the products of the RuO_4 oxidation. Additionally, higher amounts of oxygen containing species in the pyrolyzates and chemical degradation products as well as elevated IR absorptions by CO bands were observed, whereas a lower contribution of aliphatic moieties was indicated by lower contribution of aliphatics in the pyrograms, lower intensities of the CH_{aliph} bands in the IR spectra and less fatty acids released by RuO_4 oxidation. Hence, the dominance of aromatic moieties as well as the elevated insertion of oxygen can be stated for the non-extractable organic matter linked with this maceral group. These results supported conclusions formerly reported (Hatcher, 1990; van Krevelen, 1993; Ward and Gurba, 1999). Notably, woody material is the dominant plant material in vitrinite. Hence, evidence for lignin related material has to be attributed to vitrinite rich samples. Methoxy/methyl substituted benzoic acids released by TMAH-thermochemolysis were reported to be indicative for lignin related macromolecular material (Hatcher et al., 1992, 1995). However, in our sample set no correlation was observed for the appearance of these compounds in TMAH-thermochemolysis products or BBr_3 treatment products. Furthermore, high relative amounts of phenol, also formerly characterized to be a lignin indicator (Faix et al., 1987; Iglesias and Jimenez, 2000), do not correlate with vitrinite content, but are suggested to be derived from sporopollenin as explained below. Therefore, no clear molecular indicator for the presence of lignin derived geopolymers was identified within this sample set. However, the degree of aromaticity seemed to be linked with formerly woody material represented by high vitrinite contents.

Interestingly, the chemical composition of inertinite rich coal samples (CP1 and CP2, inertinite content around 75%) as reflected by pyrolysis, FTIR analyses or chemical degradation techniques did not differ significantly as compared to vitrinite rich samples. This observation supported the above stated chemical similarity of the maceral groups vitrinite and inertinite.

These correlations for samples characterized by dominance of just one maceral group illustrate very well the usefulness of combined analytical and petrographical analyses to characterize the non-extractable organic matter in more detail. However, most samples are characterised by major contributions of at least two maceral groups and results are more difficult to interpret. In conclusion, although maceral composition significantly influences the chemical properties of macromolecular organic matter in coals and coaly fossils often, only a mixed signal was observed reflecting the complex superimposition of different plant material. In addition, even though the fossils and coal samples originated from different palaeogeographical locations and flora realms (see Armstroff et al., 2006-this volume) they show a very similar macromolecular composition.

A second factor influencing the chemical quality of coal material is the degree of thermal maturity. Since most of the significant correlations observed could be attributed to the state of thermal maturity as reflected by vitrinite reflectance or T_{max} values, maturity effects have to be regarded as dominant for the chemical composition of the Palaeozoic coals investigated. Particularly, the aromatisation and the loss of oxygen containing functional groups are reflected by significant correlations of vitrinite reflectance and corresponding results of FTIR analysis (e.g. CH_{arom}/CH_{aliph}, CH_{arom}, CO, CO/CH_{arom}), pyrolysis (e.g. Oxyg/Benz,) and TMAH thermochemolysis (e.g. methylmethoxybenzoic acids). These observations illustrate the necessity to consider the thermal maturity for interpretation of chemical characterisations of Palaeozoic coals. Clearly, maturity related trends were more significant in the samples investigated than trends of chemical composition with either maceral composition or age. Additionally, in case of maceral compositions and time trends, as discussed in the following, no correlations of vitrinite reflectance with these parameters were revealed. Hence, a superimposition of the maceral or time related trends can be excluded for the sample set of this study.

4.2. Evolutionary trends

The Palaeozoic marks a time period of a rapid development and diversification of terrestrial plants. Associated with these processes also an evolution of the biochemical inventory of land plants could be suspected. In order to find out about evolutionary developments of biogenic macromolecules on a molecular level all results obtained for the coal and fossil samples were correlated with time. The absolute ages have been calculated by moving averages according to ages given in the Stratigraphic Timescale of Germany — STD 2002 (German Stratigraphic Commission, 2002). Generally, only very few significant correlations were observed.

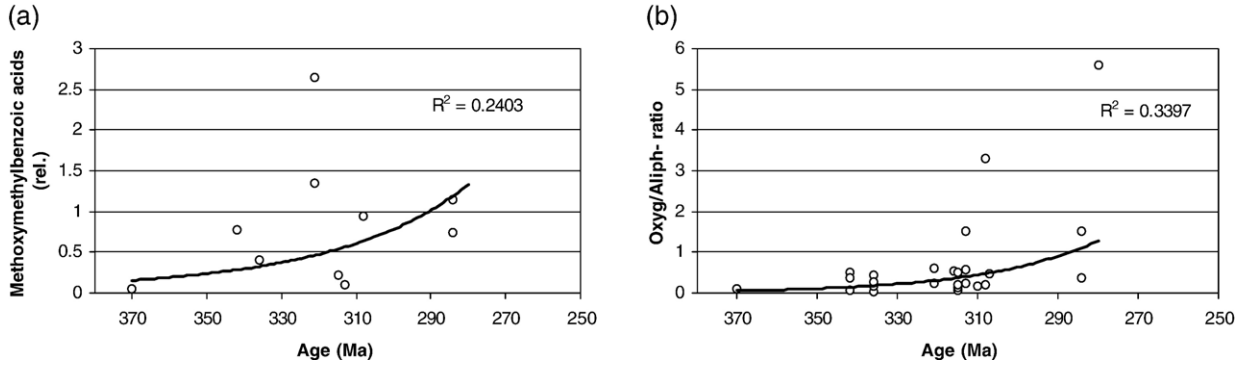

Fig. 14. Cross plots of methoxymethylbenzoic acids (a) and Oxyg/Aliph-ratio (b) and age of samples.

Chemical parameters correlate with age only with respect to oxygen containing moieties and with only minor significance (see Figs. 14 and 15). Pyrolytic results suggest a slight enrichment of phenols and fatty acids in relation to aliphatic compounds (Fig. 14b). Also a very slight increase of methoxymethylbenzoic acids derived from the TMAH-thermochemolysis with time was observed (Fig. 14a), which can be discussed to be indicative for an increasing proportion of lignin type matter. These observations are supported by results of Gottlieb (1989), who stated increasing oxygen content in lignin with ongoing evolution of land plants.

However, these observations are slightly contradicted by FTIR analyses, which revealed an decrease of CO absorption bands over time (see Fig 15). Notably, the FTIR results considered only carbonyl bands and, therefore, a direct comparison with the pyrolytic or thermochemolytic results is limited.

Beside the chemical results the petrographical characterisation over the time period investigated revealed two complementary trends. From the Devonian to the Permian a decrease of liptinite content and an increase of inertinite content are obvious.

This observation agrees with the oxygen trend discussed above. Because inertinite is characterized by higher oxygen content as compared to liptinite, a corresponding development has to be expected.

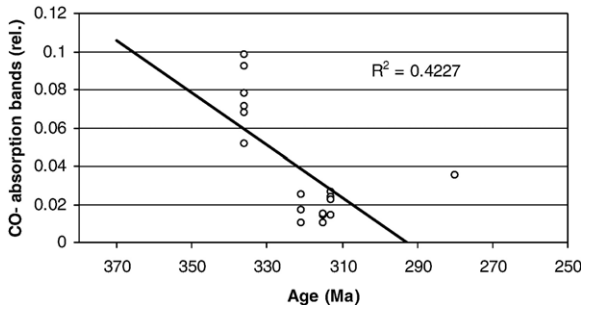

Fig. 15. Correlation between CO-absorption bands and age of samples.

Generally, the described trends of minor significance were the only correlations observed in terms of time trends. Therefore, significant changes in the time period from the Devonian to the Permian cannot be stated for the chemical or petrographical properties in the samples investigated.

Besides the lack of major evolutionary modifications, also a high similarity of Palaeozoic plant derived organic matter with recent plant material in terms of chemical composition can be assumed. The macromolecular matter of the samples investigated exhibited maceral depending chemical properties (as discussed in Section 4.1), which correspond very well with the organic polymers in more recent coals, peat and modern plant material (Jenisch et al., 1990; Hatcher et al., 1995, Hatcher and Clifford, 1997; del Rio and Hatcher, 1998; Mastalerz et al., 1998). These observations are supported by a study of Zodrow et al. (2000) which revealed that Palaeozoic organic matter possesses very similar functional groups and chemical properties as compared to recent plant material.

5. Conclusions

Considering all results discussed the following main conclusions can be drawn:

- Combining different analytical techniques allows to obtain a very detailed insight into the chemical and petrographical properties of the non-extractable organic matter of coals. Variations of both, chemical or microscopical characteristics are reflected frequently by the complementary technique. Thus, the combined application of a wide range of analytical techniques is recommended for a comprehensive characterisation of coal material.

- Thermal maturity related processes were found out to be dominant for chemical alterations. Although the thermal maturity of the samples investigated was relatively low (VR_r lower than 0.9%) a major part of specific chemical information on the macromolecular organic matter has been lost during diagenesis.
- A biochemical development of land plant material with respect to the macromolecular fraction could not be observed. Thus, the rapid morphologic evolution of higher land plants in the Late Palaeozoic is not reflected in a significant way by the chemical composition of the non-extractable matter in the coal samples investigated.
- It has to be assumed that the macromolecular organic matter of land plants in the Devonian to Permian period did not differ significantly as compared to modern land plant material. Hence, it has to be discussed, whether a biochemical evolution of the macromolecular material, which allowed to build up the floristic realm of higher land plants, has to be allocated to a time period before the Devonian/Carboniferous.

Acknowledgement

We would like to thank H. Kerp and W. Peters-Kottig (University of Muenster), C. Wheatley (British Geological Survey), J.A. Bojesen-Koefoed (GEUS Denmark), F. Koerner and J. Schneider (University of Freiberg), C. Hartkopf-Froeder (Geologischer Dienst NRW) for sample material and geological background information. Y. Esser, B. Gieren and R. Mildenberger are thanked for technical assistance with the analytical work. This project was funded by Deutsche Forschungsgemeinschaft DFG (grant Li618/5) as part of the priority programme 1054 (Evolution of the system earth in the Late Palaeozoic—clues from sediment geochemistry). The manuscript benefited greatly from editorial comments by Claude Largeau (CNRS/ENSCP, Paris) and Lorenz Schwark (University of Cologne).

References

Alekseev, A.S., Konova, L.I., Nikishin, A.M., 1996. The Devonian and Carboniferous of the Moscow Syneclise (Russian Platform): stratigraphy and sea-level changes. Tectonophysics 268, 149–168.

Armstroff, A., Wilkes, H., Gieren, B., Schwarzbauer, J., Littke, R., Horsfield, B., 2006. Aromatic hydrocarbon biomarkers in terrestrial organic matter of Devonian to Permian age. Palaeogeography, Palaeoclimatology, Palaeoecology, vol. 240, pp. 253–274. [this volume].

Béhar, F., Hatcher, P.G., 1995. Artificial coalification of a fossil wood from brown coal by confined system pyrolysis. Energy and Fuels 9, 984–994.

Blanc, P., Albrecht, P., 1990. Molecular markers in bitumen and macromolecular matrix of coals: their evaluation as rank parameters. In: Charcosset, H. (Ed.), Advanced Methodologies in Coal Characterizations. Coal Science and Technology Series, vol. 15. Elsevier, pp. 37–66.

Boucher, R.J., Standen, G., Eglinton, G., 1991. Molecular characterization of kerogens by mild selective chemical degradation–ruthenium tetroxide oxidation. Fuel 70, 695–702.

Bracewell, J.M., Robertson, G.W., 1980. Pyrolysis-mass spectrometry studies of humification in a peat and a peaty podzol. Journal of Analytic and Applied Pyrolysis 2, 53–62.

Caallinor, J.M., 1989. A pyrolysis-derivatisation-gas chromatograph technique for the elucidation of some synthetic polymers. Journal of Analytic and Applied Pyrolysis 18, 233–244.

Camarero, S., Galletti, G.C., Martinez, A.T., 1994. Preferential degradation of phenolic lignin units by two white rot fungi. Applied and Environmental Microbiology 60 (12), 4509–4516.

Chaloner, W.G., Meyen, S.V., 1973. Carboniferous and Permian floras on the northern continents. In: Hallam, A. (Ed.), Atlas of Palaeobiogeography. Elsevier, Amsterdam, pp. 169–186.

Choi, C., Wang, S.H., Stock, L.M., 1988. Ruthenium tetroxide catalyzed oxidation of maceral groups. Energy and Fuels 2, 37–48.

Collinson, M.E., van Bergen, P.F., Scott, A.C., de Leeuw, J.W., 1994. The oil-generating potential of plants from coal and coal-bearing strata through time: a review with new evidence from Carboniferous plants. In: Scott, C., Fleet, A.J. (Eds.), Coal and Coal-Bearing Strata as Oil-Prone Source RocksGeological Society Special Publication, pp. 31–70.

Cranwell, P.A., 1981. Diagenesis of free and bound lipids in terrestrial detritus deposited in a lacustrine sediment. Organic Geochemistry 3, 79–89.

del Rio, J.C., Hatcher, P.G., 1998. Analysis of aliphatic biopolymers using thermochemolysis with tetramethylammonium hydroxide (TMAH) and gas chromatography–mass spectrometry. Organic Geochemistry 29, 1441–1451.

del Rio, J.C., McKinney, D.E., Knicker, H., Nanny, M.A., Minard, R.D., Hatcher, P.G., 1998. Structural characterization of bio- and geo-macromolecules by off-line thermochemolysis with tetramethylammonium hydroxide. Journal of Chromatography A 823, 433–448.

Disnar, J.R., Harouna, M., 1994. Biological origin of tetracyclic diterpanes, *n*-alkanes and other biomarkers found in Lower Carboniferous Gondwana coals (Niger). Organic Geochemistry 21, 143–152.

Erdmann, J.G., 1965a. Petroleum — its origin in the earth. In: Young, A., Galley, J.E. (Eds.), Fluids in Subsurface Environments 4, Am. Assoc. Petr. Geol. Memoir, pp. 20–52.

Erdmann, J.G., 1965b. The molecular complex comprising heavy petroleum fractions. Hydrocarbon Analysis, vol. 389. ASTM Spec. Tech. Publ., pp. 259–300.

Espitalié, J., Durand, B., Roussel, J.C., Souron, C., 1973. Etude de la matiére organique insoluble (kerogene) des argiles du Toarcien du bassin de Paris : II, Etudes en spectroscopie infrarouge, en analyse thermique differentielle et en analyse thermogravimétrique. Revue de l'Institut Français du Pétrole 28, 37–66.

Espitalié, J., Laporte, J.L., Madec, M., Marquis, F., Leplat, P., Paulet, J., Boutefou, A., 1977. Méthode rapide de caractérisation des roches méres, de leur potentiel pétrolier et leur degré d´évolution. Revue de l'Institut Français du Pétrole 40, 536–579.

Ewbank, G., Edwards, D., Abbott, G.D., 1996. Chemical characterization of Lower Devonian plants. Organic Geochemistry 25, 461–473.

Fabianska, M.J., Kruszewska, K.K.J., 2003. Relationship between petrographic and geochemical characterisation of selected South African coals. International Journal of Coal Geology 54, 95–114.

Faix, O., Meier, D., Grobe, I., 1987. Studies on isolated lignins and lignins in woody materials by pyrolysis-gas chromatography–mass spectrometry and off-line pyrolysis-gas chromatography with flame ionization detection. Journal of Analytic and Applied Pyrolysis 11, 403–416.

Filley, T.R., Minard, R.D., Hatcher, P.G., 1999. Tetramethylammonium hydroxide (TMAH) thermochemolysis: proposed mechanisms based upon the application of ^{13}C-labeled TMAH to a synthetic model lignin dimmer. Organic Geochemistry 30, 607–621.

Galletti, G.C., Bocchini, 1995. Pyrolysis/gas chromatography/mass spectrometry of lignocellulose. Rapid Communications in Mass Spectrometry 9, 815–826.

Garcette-Lepecq, A., Derenne, S., Largeau, C., Bouloubassi, I., Saliot, A., 2000. Origin and formation pathways of kerogen-like organic matter in recent sediments off the Danube Delta (northwestern Black Sea). Organic Geochemistry 31, 1663–1683.

Gelin, F., Boogers, I., Noordeloos, A.A.M., Sinninghe Damste, J.S., Riegman, R., de Leeuw, J.W., 1997. Resistant biomacromolecules in marine microalgae of the classes Eustigmatophyceae and Chlorophyceae: geochemical implications. Organic Geochemistry 26, 659–675.

German Stratigraphic Commission (Ed.), 2002. Stratigraphic Table of Germany 2002.

Goni, M.A., Nelson, B., Blanchette, R.A., Hedges, J.I., 1993. Fungal degradation of wood lignins: geochemical perspectives from CuO-derived phenolic dimers and monomers. Geochimica et Cosmochimica Acta 57, 3985–4002.

Gottlieb, O.R., 1989. The role of oxygen in phytochemical evolution towards diversity. Phytochemistry 28, 2545–2558.

Grasset, L., Amblès, A., 1998. Aliphatic lipids released from a soil humin after enzymatic degradation of cellulose. Organic Geochemistry 29, 893–897.

Guo, Y., Bustin, R.M., 1998. FTIR spectroscopy and reflectance of modern charcoals and fungal decayed wood: implications for studies of inertinite in coals. International Journal of Coal Geology 37, 29–53.

Han, Z., Kruge, M.A., 1999. Chemistry of maceral and groundmass density fractions of torbanite and cannel coal. Organic Geochemistry 30, 1381–1401.

Hatcher, P.G., 1990. Chemical structural model for coalified wood (vitrinite) in low rank coal. Organic Geochemistry 16, 959–968.

Hatcher, P.G., Clifford, D.J., 1994. Flash pyrolysis and in situ methylation of humic acids from soil. Organic Geochemistry 21, 1081–1092.

Hatcher, P.G., Clifford, D.J., 1997. The organic geochemistry of coal: from plant materials to coal. Organic Geochemistry 27, 251–274.

Hatcher, P.G., Faulon, J.-P., Wenzel, K.A., Cody, G.D., 1992. A structural model for lignin-derived vitrinite from high-volatile coal (coalified wood). Energy and Fuels 6, 813–820.

Hatcher, P.G., Nanny, M.A., Minard, R.D., Dible, S.D., Carson, D.M., 1995. Comparison of two thermochemolytic methods for the analysis of lignin in decomposing gymnosperm wood: the CuO oxidation method and the method of thermochemolysis with tetramethylammonium hydroxide (TMAH). Organic Geochemistry 23, 881–888.

Hayatsu, R., Botto, R.E., Mcbeth, R.L., Scott, R.G., Winans, R.E., 1988. Chemical alteration of a biological polymer "sporopollenin" during coalification: origin, formation, and transfromation of the coal maceral sporinite. Energy and Fuels 2, 843–847.

Hedges, J.I., Mann, D.C., 1979. The characterization of plant tissues by their lignin oxidation products. Geochimica et Cosmochimica Acta 43, 1803–1807.

Horsfield, B., 1989. Practical criteria for classifying kerogens: some observations from pyrolysis-gas chromatography. Geochimica et Cosmochimica Acta 53, 891–901.

Iglesias, M.J., Jimenez, A., 2000. Molecular characterisation of vitrinite in relation to natural hydrogen enrichment and depositional environment. Organic Geochemistry 31, 1285–1299.

Ikeya, K., Yamamoto, S., Watanabe, A., 2004. Semiquantitative GC/MS analysis of thermochemolysis products of soil humic acids with various degrees of humificaion. Organic Geochemistry 35, 583–594.

Jenisch, A., Richnow, H.H., Michaelis, W., 1990. Chemical structural units of macromolecular coal components. Organic Geochemistry 16, 917–929.

King, L.H., Goodspeed, F.E., Montgomery, D.S., 1963. Study of Sedimented Organic Matter and Its Natural Derivatives. Mines Branch Report R, vol. 114. Dept. Mines Techn. Surv., Ottawa.

Kögel-Knabner, I., 2000. Analytical approaches for characterizing soil organic matter. Organic Geochemistry 31, 609–626.

van Krevelen, D.W., 1993. Coal-Typology, Physics, Chemistry, Constitution. Elsevier, Amsterdam.

Largeau, C., Derenne, S., Casadevall, E., Kadouri, A., Sellier, N., 1986. Pyrolysis of immature Torbanite and the resistant biopolymer (PRB A) isolated from extantalga Botryoccocus braunii. Mechanism of formation and structure of Torbanite. In: Leythaeuser, D., Rullkötter, J. (Eds.), Advances in Organic Geochemistry 1985. Organic Geochemistry, vol. 10. Pergamon Press, Oxford, pp. 1023–1032.

Littke, R., ten Haven, H.L., 1989. Paleoecologic trends and petroleum potential of Upper Carboniferous coal seams of Western Germany as revealed by their petrogaphic and organic geochemical characteristics. In: Lyons, P.C., Alpern, B. (Eds.), Peat and Coal 1, Origin, Facies and Depositional ModelsInternational Journal of Coal Geology, vol. 13, pp. 529–574.

Littke, R., Horsfield, B., Leythaeuser, D., 1989. Hydrocarbon distribution in coals and dispersed organic matter of different maceral composition and maturities. Geologische Rundschau 78, 391–410.

Martin, F., del Rio, J.C., Gonzáles, F.J., Verdejo, T., 1995. Pyrolysis derivatisation of humic substances. 2. Pyrolysis of soil units in the presents of tetrametylammoniumhydroxide. Journal of Analytic and Applied Pyrolysis 31, 75–83.

Mastalerz, M., Hower, J.C., Carmo, A., 1998. In situ FTIR and flash pyrolysis/GC–MS characterization of Protosalvinia (Upper Devonian, Kentucky, USA): implications for maceral classification. Organic Geochemistry 28, 57–66.

McKinney, D.E., Carson, D.M., Clifford, D.J., Minard, R.D., Hatcher, P.G., 1995. Off-line thermochemolysis versus flash pyrolysis for the in situ methylation of lignin: is pyrolysis necessary? Journal of Analytic and Applied Pyrolysis 34, 41–46.

Meyer-Berthaud, B., Schleckert, S.E., Wendt, J., 1999. *Archaeopteris* is the earliest known modern tree. Nature 398, 700–701.

Moldowan, J.M., Dahl, J., Huizinga, B.J., Fago, F.J., Hickey, L.J., Peakman, T.M., Taylor, D.W., 1994. The molecular fossil record of oleanane and its relation to angiosperms. Science 265, 768–771.

Mongenot, T., Derenne, S., Largeau, C., Tribovillard, N.-P., Lallier-Vergés, E., Dessort, D., Connan, J., 1999. Spectroscopic, kinetic and pyrolytic studies of kerogen from the dark parallel laminae facies of the sulphur-rich Orbagnoux deposit (Upper Kimmeridgian, Jura). Organic Geochemistry 30, 39–56.

Mösle, B., Finch, P., Collinson, M.E., Scott, A.C., 1997. Comparison of modern and fossil plant cuticles by selective chemical extraction

monitored by flash pyrolysis-gas chromatography–mass spectrometry and electron microscopy. Journal of Analytical and Applied Pyrolysis 40–41, 585–597.

Mösle, B., Collinson, M.E., Scott, A.C., Finch, P., 2002. Chemosystematic and microstructural investigations on Carboniferous seed plant cuticles from four North American localities. Review of Palaeobotany and Palynology 120, 41–52.

Myke, B., Michaelis, W., 1986. Lignin-derived molecular fossils from geological materials. Naturwissenschaften 73, 731–734.

Naafs, D.F.W., van Bergen, P.F., 2002. A qualitative study on the chemical composition of ester-bound moieties in an acidic andosolic forest soil. Organic Geochemistry 33, 189–199.

Nip, M., Tegelaar, H., Brinkhuis, H., de Leeuw, J.W., Schenck, P.A., Holloway, P.J., 1986. Analysis of modern and fossil plant cuticules by Curie point Py–GC and Curie point-GC–MS: recognition of a new, highly aliphatic and resistant biopolymer. Organic Geochemistry 10, 769–778.

Orem, W.H., Colman, S.M., Lerch, H.E., 1997. Lignin phenols in sediments of Lake Baikal, Siberia: application to paleoenvironmental studies. Organic Geochemistry 27, 153–172.

Ping'an Peng, Morales-Izquierdo, A., Hogg, A., Strausz, O.P., 1997. Molecular structure of Athabasca asphaltene: sulfide, ether, and ester linkages. Energy and Fuels 11, 1171–1187.

Quénéa, et al., 2005. Organic Geochemistry 36, 349–362.

Riboulleau, A., Derenne, S., Sarret, G., Largeau, C., Baudin, F., Connan, J., 2000. Pyrolytic and spectroscopic study of a sulphur-rich kerogen from the "Kashpir oil shales" (Upper Jurassic Russian platform). Organic Geochemistry 1641–1661.

Richnow, H.H., Seifert, R., Hefter, J., Kästner, M., Mahro, B., Michaelis, W., 1994. Metabolites of xenobiotica and mineral oil constituent linked to macromolecular organic matter in polluted environments. Organic Geochemistry 22, 671–681.

Robin, P.L., Rouxhet, P.G., 1976. Contribution des différentes functions chimiques dans les bandes d´absorption infrarouge des kérogenes situées à 1710, 1630 et 3430 cm^{-1}. Revue de l'Institut Français du Pétrole 31, 955–977.

Scheidt, G., Littke, R., 1989. Comparative organic petrology of interlayed sandstones, siltstones, mudstones and coals in the Upper Carboniferous Ruhr Basin, Northwest Germany, and their thermal history and methane generation. Geologische Rundschau 78, 375–390.

Schenk, H.J., Witte, E.G., Littke, R., Schwochau, K., 1990. Structural modifications of vitrinite and alginite concentrates during pyrolytic maturation at different heating rates. A combined infrared, ^{13}C NMR and microscopical study. Organic Geochemistry 16, 943–950.

Schulze, T., Michaelis, W., 1989. Structure and origin of terpenoid hydrocarbons in some German Coals. Organic Geochemistry 16, 749–761.

Schulten, H.R., Leinweber, P., 1995. Characterisation of humic and soil particles by analytical pyrolysis and computer modelling. Journal of Analytic and Applied Pyrolysis 38, 1–53.

Schwarzbauer, J., Ricking, M., Gieren, B., Keller, R., Littke, R., 2005. Anthropogenic organic contaminants incorporated into the non-extractable particulate matter of riverine sediments from the Teltow Canal (Berlin). In: Lichtfouse, Schwarzbauer, Robert (Eds.), Environmental Chemistry. Springer Verlag, Weinheim, pp. 329–352.

Silva, M., Kalkreuth, W., 2005. Petrological and geochemical characterization of Candiota coal seams, Brazil — implication for coal facies interpretations and coal rank. International Journal of Coal Geology 64, 217–238.

Simpson, M.J., Hatcher, P.G., 2004. Determination of black carbon in natural organic matter by chemical oxidation and solid-state ^{13}C nuclear magnetic resonance spectroscopy. Organic Geochemistry 35, 923–935.

Stankiewicz, B.A., Kruge, M.A., Mastalerz, M., 1996. A geochemical study of macerals from a Miocene lignite and Eocene bituminous coal, Indonesia. Organic Geochemistry 24, 531–545.

Stankiewicz, B.A., Scott, A.C., Collinson, M.E., Finch, P., Mösle, B., Briggs, D.E.G., Evershed, R.P., 1998. Molecular taphonomy of arthropod and plant cuticles from the Carboniferous of North America: implications for the origin of kerogen. Journal of the Geological Society 155, 453–462.

Stock, L.M., Wang, S.-H., 1985. Ruthenium tetroxide catalysed oxidation of Illinois No. 6 coal. Fuel 64, 1713–1717.

Taylor, G.H., Teichmüller, M., Davis, A., Diesel, C.F.K., Littke, R., Robert, P., 1998. Organic Petrography, Gebrueder Borntraeger. Stuttgart, Berlin.

ten Haven, H.L., Littke, R., Rullkötter, J., 1992. Hydrocarbon biological markers in Carboniferous coals of different maturities. In: Moldowan, J.M., Albrecht, P., Philip, R.P. (Eds.), Biological Markers in Sediments and Petroleum. Prentice Hall, New Jersey, pp. 142–155.

Tegelaar, E.W., de Leeuw, J.W., Derenne, S., Largeau, C., 1989. A reappraisal of kerogen formation. Geochimica et Cosmochimica Acta 15, 3103–3106.

van Bergen, P.F., Scott, A.C., Barrie, P.J., de Leeuw, J.W., Collinson, M.E., 1994. The chemical composition of Upper Carboniferous pteridosperm cuticles. Organic Geochemistry 21, 107–112.

Veld, H., Fermont, W.J.J., Jegers, L.F., 1993. Organic petrological characterization of Westphalian coals from Netherlands: a correlation between Tmax, vitrinite reflectance and hydrogen index. Organic Geochemistry 20, 659–675.

Vella, A.J., Holzer, G., 1990. Ether-derived alkanes from sedimentary organic matter. Organic Geochemistry 15, 209–214.

Ward, C.R., Gurba, L.W., 1999. Chemical composition of macerals in bituminous coals of the Gunnedah Basin, Australia, using electron microprobe analysis techniques. International Journal of Coal Geology 39, 279–300.

Wiemann, R., Ahlers, F., Schmitz-Thorm, I., 2001. Sporopollenin. In: Steinbüchel, A. (Ed.), Biopolymers, vol. 1. Wiley-VCH, Weinheim, pp. 209–227.

Zhong, N.N., Smyth, M., 1997. Striking liptinic bark remains peculiar to some Late Permian Chinese coals. International Journal of Coal Geology 33, 333–349.

Zodrow, E.L., Mastalerz, M., Orem, W.H., Simunek, Z., Bashfort, A.R., 2000. Functional groups and elemental analyses of cuticular morphotypes of *Cordiates principalis* (Germany) Geinitz, Carboniferous Maritimes Basin, Canada. International Journal of Coal Geology 45, 1–19.